# THE McCOY, NEVADA GEOTHERMAL PROSPECT

*An Interim Case History*

PART I (Text)

by Arthur L. Lange

*Paper delivered at the Fiftieth Annual Meeting of the Society of Exploration Geophysicists, Houston, Texas, 17 November 1980.*

AMAX Exploration Inc.
Geothermal Branch
7100 W. 44th Avenue
Wheat Ridge, Colorado 80033

## Author's Note

Passages in brackets [ ] and footnotes were deleted during the presentation, in order to meet the time requirements

# THE McCOY, NEVADA GEOTHERMAL PROSPECT

## An Interim Case History (Abstract, revised)

by Arthur L. Lange, AMAX Exploration Inc., Geothermal Branch

The McCoy prospect is located in Lander and Churchill Counties of central Nevada, approximately 65km NW of Austin. Exploration is being conducted by AMAX Exploration, Inc. partially supported by the Department of Energy's Industry-Coupled Program. The property has been consolidated with O'Brien Resources as a Federal geothermal unit. O'Brien is also participating in the exploration program.

The geothermal area occupies the junction of the Augusta and Clan Alpine Mountains and the New Pass Range, made up of Paleozoic through Tertiary sediments, and igneous rocks. Cenozoic volcanics range in age from 36 to 16 million years. The sequence has been subjected to multiple folding and thrusting, and transected by basin-range faulting since Late Miocene time. Mercury has been sporadically produced from the McCoy Mine near the center of the prospect. One water sample was obtained from a well at the McCoy mine (39°C, 1065 TDS). The water chemistry forecasts a minimum equilibration temperature of 186°C but with a rather high deduced cold water fraction.

Temperature surveys made in 40 gradient holes and 5 existing holes resulted in a N/S-trending thermal anomaly 20km long and 3 to 5km wide. The heatflow pattern, based on thermal conductivities from cuttings, exhibits three principal centers measuring 15 (over the mine) to 22HFU (near the southern end of the anomaly).

A complete Bouguer gravity map produced from 340 stations reveals two gravity low zones forming an upright V, intersecting at the region of highest heat flow. These zones coincide with two aeromagnetic low trends.

A passive seismic survey conducted during 31 days over 22 stations detected 36 microearthquakes. Of those locatable, a cluster of 3 occurred at the McCoy mine, 3 more at the southern end of the property and 3 to the west. A P-wave delay correlates with the highest heatflow in the southeast, where Poisson's ratio reaches 0.35. An advance is mapped in the vicinity of the McCoy mine, where a Poisson's ratio of .15 occurs (typical of hot, dry rock or the dry steam reservoir at The Geysers, California).

An extensive self-potential survey resulted in a negative anomaly of 50 to 90 millivolts corresponding approximately to the thermal feature. Localized negatives appear over the McCoy mine and the thermal high to the south.

A magnetotelluric survey of 38 stations reveals (in one-dimensional inversions) a resistive section to 10 or more km depth in the vicinity of the McCoy mine. The southern region appears conductive above one kilometer, while at depth, an extended conductive zone ascends to 3km

depth in the vicinity of the highest heat flow, SP negative peak and the P-wave delay zone. The MT soundings are supplemented in the upper zones by an electromagnetic survey conducted by Lawrence Berkeley Laboratories.

Two deep gradient holes (to 600 and 750 meters) in the zones of highest heat flow encountered warm aquifers at about 500m, whose waters permeated the wells to their bottoms. An interpretation of the southeastern anomalies suggests that a deep reservoir (and possibly a heat source) communicates with the 100°C aquifer of the test well via a westward-dipping fault zone along the west side of a horst block that prevents migration of the fluids eastward.

# INTRODUCTION

The McCoy geothermal prospect was discovered during an AMAX reconnaissance program in 1977 and [first described in a preliminary report by H. Olson at the 1979 Geothermal Resources Council meeting] (Olson, et al., 1979. Located in Lander and Churchill Counties, Nevada, approximately 65km NW of Austin (SLIDE 1L), it is essentially a "blind" hydrothermal system having no surface discharge of hot waters. It differs from most Great Basin prospects in its occurrence within a range rather than the valley or its margin. Its potential was recognized from elevated temperatures measured in mineral drill holes, one water sample from a well, and the existence of mercury mines. The property has been consolidated with O'Brien Resources as a Federal geothermal unit. Exploration has been partially supported by the Department of Energy's Industry-coupled program. I would like to thank the DOE, O'Brien, and AMAX Exploration, Inc. for the opportunity to present the results thus far. The talk will review the analysis of a variety of geophysical results in the context of known and inferred geology. We shall proceed by examining a Landsat image, heat flow, gravity and magnetics, seismic properties and electrical effects.

## LOCATION AND DESCRIPTION

The geothermal area occupies the junction of the Augusta and Clan Alpine Mountains and the New Pass Range, which together separate Dixie Valley on the west from Antelope Valley on the east (SLIDES 2R, 3L). Elevations of the prospect range from about 1200m just west of the gap called Hole in the Wall to 2162m on McCoy Peak, [resulting in a variety of vegetation from that of desert brush to juniper and pinon pine forest].

Mercury has been produced sporadically from cinnabar deposits at the McCoy and Wildhorse mines (SLIDE 4L). Sodium bicarbonate water pumped from a 39$^{o}$C aquifer at 58m in a well at the McCoy mine yielded an equilibration temperature of 186$^{o}$C, [after applying an 85% deduced cold water mixing model to the silica geothermometer].

## LANDSAT FEATURES

On this portion of a Landsat image (SLIDE 5R), produced by Eureka Resources, we recognize the principal topographic features of Dixie Valley, Antelope Valley, and the three intersecting ranges: [Clan Alpine, New Pass and the Augusta Mountains]. Highway 50 from Austin is visible at New Pass. The McCoy mine lies immediately east of an evident zone of alteration. In addition to four sets of lineations recognized by geologists, Cenozoic volcanic centers are present. The Fish Creek caldera lies north of the prospect, and a clearly discernible ring feature surrounds the McCoy mine, cautiously described as an "incipient caldera." The 25-kilometer-diameter ring encompasses the juncture of the three ranges and portions of Antelope and Dixie Valleys. A pervasive, evidently deep, lineament crosses the ring in a northwestward orientation through the McCoy mine and appears to control the main drainage of the feature, emptying via Hole in the Wall into Dixie Valley, at a point due east of the SunEdco geothermal discovery well.

# GEOLOGY

During Pennsylvanian and Permian time, sediments were deposited in a rapidly subsiding eugeosyncline (SLIDES 6L, 7R). These strata, consisting of chert, volcanics, clastics, and limestone of the Havallah sequence are shown in blue on the simplified geologic map and E-W cross-section through the McCoy mine, as protrayed by H.D. Pilkington (1979).

The basal Triassic unit (TRc) (in green) is a detritus composed of conglomerate, siltstone, sandstone and minor tuff resting unconformably on the Paleozoics. This is overlain by mainly carbonate and sandstone rocks of Triassic age (also in green).

The Tertiary rocks (in red) are primarily volcanics that accumulated in lenses upon an erosion surface between 36 and 16 million years ago. These are interlayered with sediments, and broken by basin-range faulting.

A Quaternary fossil travertine mound (Qt) about 10m thick and over 2km in area overlies the Tertiary rocks northwest of the McCoy mine. In addition extensive bleaching and silicification have affected the rocks in the central portion of the prospect.

Our detailed understanding of the McCoy geology is being considerably expanded by Jos. Moore and Mike Adams of the University of Utah Research Institute whose contribution I gratefully acknowledge.

## TEMPERATURE AND HEAT FLOW

Temperature surveys made in 40 gradient holes and 5 existing holes resulted in a N/S-trending thermal anomaly 20km long and 3 to 5km wide (SLIDE 8L). The computed heatflow, based on thermal conductivities from cuttings, produces an anomaly containing three principle centers measuring between 15 (over the mine) and 23HFU (near the southern end of the anomaly).

The plot of temperature at 100m (extrapolated where necessary) essentially duplicates the pattern of heatflow (SLIDE 9L). Two deeper gradient holes (750 and 600m) were drilled this year to test the persistence of the shallow gradients to depth. Along Line B, approx E/W depth isotherms have been constructed by linear extrapolation from the measured gradients, based on the assumption of conductive heatflow.

Comparison with the accompanying geological section shows that the isotherms (disregarding the central zone of recharge) appear to assume the form of the updomed geologic block of primarily carbonates, which, if anything, would be expected to depress isotherms, because of their higher thermal conductivity.

The 600m gradient well intercepted a $60^{o}$ aquifer at 175m, whose discharge affected the well to its bottom. We, therefore, cannot validate any of the isotherms below the $60^{o}$ zone.

Line A, running north-south (SLIDE 10R), passes through the McCoy mine workings and the southern deep gradient well, where it bends southwestward towards Edwards Creek Valley. Temperature highs occur: a) at the McCoy mine, b) near the head of the drainage 4km north of the mine, c) near the midpoint, and d) over the south well. [To the southwest the isotherms drop off into alluvium of Edwards Creek Valley].

The deduced isotherms of Line C, through the southern well (SLIDE 11R), are inclined with the bedding on the west and even pull up on the upthrown block at the left edge. To the east they plunge steeply at the zone of faulting associated with the eastern margin of the ring. Note that the horst blocks on the east interrupt the sequence of inclined Triassic sediments and, evidently, the thermal anomaly as well.

In our southern drill hole the high near-surface temperature gradient of over 400°C/km asymptoted at 475m where an aquifer of 100° water was intercepted in the Triassic conglomerate. As in the northern well, this fluid permeated the column to the bottom resulting in an apparent temperature inversion; and again the test for a continuing conductive thermal regime is inconclusive.

A very similar isotherm profile was found by Chapman, Kilty and Mase (1978) at Red Hill Hot Spring, Monroe, Utah (SLIDE 12L). There the hot water ascends along a steeply dipping fault zone on the east to discharge at the surface and thence drain westward as underflow in sediments of the adjoining basin. In our case, the fluid may ascend from Paleozoic rocks along the west edge of the horst barrier to discharge into the basal conglomerate without breaking out onto the surface. Thence it may drain using the avenue of the conglomerate passing the south well in its downdip course southwestward towards the valley.

# GRAVITY

A gravity survey of 340 stations was conducted by Microgeophysics Corporation and AMAX (SLIDES 13L, 14R). The complete Bouguer map reveals two gravity low zones forming an upright V, intersecting near the southern thermal anomaly and merging with lows of the Edwards Creek Valley. Fred Berkman has prepared two-layer depth profiles using a USGS automatic inversion program. On Line B we can recognize the less dense volcanic fill ($2.1 gm/cm^3$) near the center of the ring, where the denser carbonates (2.8) plot out at depths down to one kilometer. The dense rocks correctly plot to the surface over the upraised block at the McCoy mine, and again dip under the volcanics and thin alluvium of Antelope Valley to the east.

On Line C (SLIDE 15R) the volcanic cover thins as we move eastward across the drill site and, at a point 2km east of the well, a mass of low density material coincides with a mapped subsidence block. It appears to be much deeper than the geologically deduced graben, but what its relationship to the geothermal system may be, we are still not certain. Gravity contributed to our understanding of subsurface geology at intermediate depths, but revealed no deep heat source or reservoir.

## MAGNETICS

An aeromagnetic survey was flown at 2440m (8000ft) by Geometrix (SLIDE 16L). Like the gravity survey it yielded a V-shaped low whose juncture falls about over the southern thermal anomaly, and extends from there southward into Edwards Creek Valley.

As in the case of gravity, analysis of the magnetics has primarily mapped the Paleozoic surface but has provided no apparent clues to the existence of a geothermal reservoir or heat source.

## PASSIVE SEISMIC SURVEYS

Microgeophysics Corporation conducted a 31-day survey, recording both microearthquakes and teleseisms (SLIDE 17R). P-wave delays, which have been used to map magma chambers under volcanos and zones of partial melt beneath geothermal areas (Iyer, 1980), used arrival times from each of 9 distant earthquakes to produce the map representing P-wave delay anomalies. Travel-time residuals are depicted in terms of depth to a hypothetical boundary separating an upper slow medium from a lower one of higher velocity. [This is merely an artifice for convenient representation of delays; the retarding medium might actually be a deeply buried zone overlain by higher velocity material].

An evident zone of slow velocity material (in red) underlies the New Pass Range, as recognized from delays of 2 events on three stations. Two microearthquakes of around 3.5km depth occurred over this medium. High velocity zones (in blue) appear to underlie a block immediately south of the McCoy mine, as well as a large area covered by rhyolite flows to the west.

### Microearthquakes

Microearthquakes are commonly associated with geothermal areas (Ward, 1972). Of 36 events recorded during the McCoy survey (SLIDE 18L), sixteen fell within the boundaries of our map, including a cluster of 3 near the McCoy mine area, 3 at the northern extremity of Edwards Creek Valley, and 3 south of Hole in the Wall.

Poisson's ratio, shown by the dashed line in the profile (SLIDE 19R), is a rock property relating compressional wave velocity to that of the shear wave. Roughly, the higher the ratio of P to S velocity, the higher the Poisson's ratio.

Ratios in excess of 0.35 computed from local events are observed in the valleys (green) and probably relate to saturated alluvium. A high appears over the limestones of the Augusta Mountains to the north and also in the vicinity of our north well on Line B, where it accompanies a locally high P-wave velocity (solid curve). As we know from the well, the Augusta Mountains limestone contains water. A ratio of less than 0.15 (red) is seen over the central volcanic fill region and can be followed eastward to the McCoy mine horst block, also a region of high P-velocity. This value indicates dry, very competent material and is equivalent to that seen over the Geysers by Gupta, et al. (1980).

Along Line C, (SLIDE 20R) Poisson's ratio (dashed) is about average everywhere except over the horst blocks to the east, where it exceeds 0.35. Immediately west of the uplifted block P-wave delays (solid) reaching 210 milliseconds occupy the zone of high heatflow at the well. To the west, the P-arrivals come in early as we ascend the uplifted blocks of McCoy Peak.

Profile A (SLIDE 21R) ties together the two thermal zones: on the north, the high velocities but low Poisson's ratio over the thermal high at the McCoy mine; and on the south, the considerable P-wave slowing in a region where a normal Poisson's ratio gradually increases towards Edwards Creek Valley.

## SELF POTENTIAL

The principal self potential effects that one may expect to find in a geothermal area are 1) thermoelectric, in which electric potential differences result from temperature gradients: 2) electrokinetic, or streaming potential, due to fluid movement through pores or cracks; and 3) electrochemical, resulting from oxidation and reduction in groundwater around mineralized conductors (Corwin & Hoover, 1979). Commonly, in a geothermal area, circulating hot and cold fluids, high temperature gradients, alteration and mineralization are all present, resulting in compound self potential anomalies difficult to resolve.

A self potential survey was performed by Microgeophysics Corporation along the dotted lines of the map (SLIDES 22L, 23R). Station spacing varied between 50 and 200m, depending on voltage gradients, and 1000m wires were used. The east-west lines were run along section lines and tied with 4 north-south lines.

Positive anomalies are shown (on the left) by the orange to red colors and negatives by green, blue to grey. The area of volcanic fill in the southwest appears generally positive. As we cross the deep structure underlying Hole in the Wall wash the potentials go increasingly negative on the Augusta Mountain block probably due to hydraulic gradients.

The most striking SP effect is the hour-glass negative corresponding to the thermal anomaly shown on the right, leading me to believe that the thermeolectric effect plays a significant role at McCoy.

I have chosen to display the SP profiles along with those of temperature (SLIDE 24R). Note the overall shapes of the two anomalies. Immediately west of the well, a normal fault that abuts volcanics against

Triassic rocks bounds the thermal anomaly and results in a conspicuous dipolar SP expression. On the east limb of the dome a series of faults give rise to a step-wise SP profile and the dipolar feature seen. At the McCoy mine a sharp negative of 75mv overlies the most fractured zone of the dome, as well as a microearthquake focus, leading me to suspect that the zone is permeable. The negative spike very well may represent a mineralization anomaly superimposed on the much broader thermal effect.

The same anomaly appears on the north-south Line A (SLIDE 25R). Additional SP negative peaks or dipolar anomalies occupy the zone around the mine. Southward the SP remains rather uniformly negative until the southern heatflow high is encountered where again a strong negative appears. This spike is evident on Line C (SLIDE 26R) where it enhances the broader negative over the thermal zone. The microearthquakes project onto this region of the line--made up of fractured blocks of Paleozoics--where we earlier deduced that ascending hot water might produce the steep isotherms. Note the similarity of the shapes of the two anomalies (though one is upside-down).* I believe that in general this southern SP anomaly reflects not only the elevated temperatures measured, but as well a conduit, dipping steeply westward to a deeper thermal system.

*The SP response has the asymmetrical character of a positive anomaly modelled by Zablocki (1976) for a 45° westward dipping steam conduit at Kilauea. Though, normally, ascending fluids seem to generate positive electrokinetic anomalies, I am assured by R. Corwin, that in certain environments, negatives are possible. Alternatively, the fractures might also serve as a recharge zone near-surface, or alternate upward and downward circulation along the fault plane.

## MAGNETOTELLURICS and ELECTROMAGNETICS

A tensor MT survey was run by Terraphysics during February 1980 (SLIDE 27L). [The 3 magnetic field components were detected by a cryogenic magnetometer at base stations that included also two orthogonal electric dipoles. One or two satellite stations, consisting of dipole pairs, were telemetered back to the base and used as remote reference signals for noise reduction. The remotes were seldom more than 2km distant from the base.] Frequencies between .01 and 10hz were recorded. Terraphysics applied the well known Bostick 1-D. inversion, as a first approximation. Here we view resistivity as deduced at 5km depth.

The principal conductive anomaly (in red) appears on 5 or 6 stations beneath the southern thermal zone, and is bounded on the east and northwest blocks (blue to grey). A second conductive anomaly appears to the west in the vicinity of Hole in the Wall.

A profile of the 1D inversion of the $T_e$ mode, displays resistivity vs. a linear depth scale on Line B (SLIDE 28R). Here we see a conductive zone at 3km in the vicinity of Hole in the Wall. Eastward we encounter a very resistive zone under the thermal anomaly. The increasing thickness of volcanics and alluvium toward Antelope Valley are detected. Microearthquakes fall in the gaps of highly skewed zones.

Lawrence Berkeley Laboratories operated their EM-60 electromagnetic system over portions of Lines A and B, and they have kindly permitted me to show some preliminary results. In this comparison, the resistivities computed from the two surveys tend to merge; both detected the wedge-shaped volcanics to the east as lower resistivities. The MT highs over the dome are confirmed by the EM at least within the upper kilometer.

The prevalence of extreme resistivity changes is seen again along Line A (SLIDE 29R) where the $T_e$ and $T_m$ modes diverged systematically. Over the central resistive block, electrical strike has rotated from north-south to east-west, so that three-dimensional modelling is called for. Here again, the EM profile confirms the resistive nature of the rotated block, and reveals a veneer of conductive alteration. In the vicinity of the south hole, the MT below 1km appears conductive, reaching less than 1$\Omega$m at 7km. In the southernmost sounding, the EM began to sense this deeper conductive zone.

Line C shows conformity in the short periods between $T_e$ and $T_m$ responses shown here in pseudosection (SLIDE 30R); however, the apparent deep contact in the $T_e$ pseudosection is "not evident" in the $T_m$, suggesting the presence of a conductive narrow dike-like feature. The corresponding 1D inversion of $T_e$ (SLIDE 31R1) emphasizes the vertical conductor and an associated deep conductor. Microearthquakes project onto the line in the contact zone.

A resistivity log of the drill hole provides a comparison for confirmatory evidence for the MT and EM results. Resistivities oscillate between about 32 and 500$\Omega$m in the log. MT resistivity averages 24$\Omega$m, while the EM ranges from 9 to 1500$\Omega$m .

M. Wilt of LBL assisted me in generating several 2D models of the MT data on Line C using a modified version of the Vozoff-Swift-Madden program. By introducing a conductive dike along a contact and a conductive zone on the west side at depth (approximately what we see in the 1D inversion) we are able to reproduce the gross features of the two pseudosections, although not the exact resistivities and dimensions.

# SYNTHESIS

The various geophysical surveys have yielded distributions of rock properties resulting in what I call an "anomaly sandwich". I shall concentrate on the area of the known thermal anomaly shown on the heat flow map (SLIDE 32L). The northern portion of the anomaly is an upraised block made up of dense Triassic and Paleozoic sediments, altered and possibly silicified. It exhibits a P-wave advance and Poisson's ratio ranging from very high northwest of the McCoy mine to very low over the remainder. A self-potential negative occurs over electrically resistive material. Thus, the block seems to be hot and dry on the south and east, but contains water to the northwest, as our drillhole confirmed. We see no underlying deep conductor in the MT sections that might correspond to a liquid-dominated reservoir or magmatic heat source.

The southern portion of the thermal anomaly is underlain by a similar arching of Paleozoic and Triassic rocks where two gravity and magnetic troughs converge. The Poisson's ratio increases eastward from normal to 0.35 and a large P-wave delay underlies the southeast quadrant. The thermal high exhibits a negative self potential and an MT-conductive medium below 3 or 4km bounded by a resistive block on the east. High concentrations of mercury were reported from two wells by J. Moore of UURI. Along the resistivity boundary, [1.5km east of the drill site,] there appears a narrow conductive feature, aligned with a self-potential negative peak, microearthquake foci, and plunging isotherms.

In cross-section along Line C (SLIDE 33R), my interpretation is the following: In the MT and P-wave delay profiles we see a deep reservoir at 3 or more kilometers, possibly heated by an intrusive and delivering hot

fluids to fault conduits bounding a horst block. These encounter the Triassic conglomerate where they become mixed with meteoric water entering the permeable zone from the surface. The mixture drains southwestward following the conglomerate, passing through our drill hole at a temperature of 100°c. The water returns to the system by whatever avenues exist downdip. Occasional seismicity insures that the path of ascending fluid remains fractured and open.

[In summary, seismic, electrical and temperature surveys contributed valuable insight into the nature of the geothermal anomaly at McCoy. Gravity and magnetics helped our understanding of the geology. In the future, dipole-dipole resistivity lines are planned to supplement the EM and MT results, while additional intermediate-depth temperature holes are being scheduled to test the interpretations presented here.]

## REFERENCES


CHAPMAN, D.S., K.T. KILTY & C.W. MASE (1978). Temperatures and their dependence on groundwater flow in shallow geothermal systems. *Geothermal Resources Transactions* 2 (2): 79-82.

CORWIN, R.F. & D.B. HOOVER (1979). The self potential method in geothermal exploration. *Geophysics* 44 (2): 226-245.

GUPTA, H.K., T.L. LIN & R.W. WARD (1980). Investigation of the seismic wave velocities at The Geysers geothermal field, California. *Geothermal Resources Council Transactions* 4: 57-60.

IYER, H.M. (1980). Magma Chambers and geothermal energy. *Paper at 50th Annual Meeting of Society of Exploration Geophysicists, Houston:* GT-6.

OLSON, H.J., F. DELLECHAIE, H.D. PILKINGTON & A.L. LANGE (1979). The McCoy geothermal prospect: A status report of a possible new discovery in Churchill and Lander Counties, Nevada. *Geothermal Resources Council Transactions* 3: 515-518.

PILKINGTON, H.D. (1979). Geology of the McCoy area, Nevada. AMAX Exploration Inc. (Ms.). 19p, 1 fig., 7 pl.

WARD, PETER L. (1972). Microearthquakes: Prospecting tool and possible hazard in the development of geothermal resources. *Geothermics* 1: 3-12.

ZABLOCKI, CHAS. J. (1976). Mapping thermal anomalies on an active volcano by the self-potential method, Kilauea, Hawaii. *U.S. Geological Survey, Hawaiian Volcano Observatory, Report:* p. 1299-1309.


## CONTRACTOR REPORTS


MICROGEOPHYSICS CORP. (1980). *McCoy, Nevada Gravity Survey.* Report prepared for AMAX Exploration Inc. 1 January 1980.

MICROGEOPHYSICS CORP. (1979). *McCoy, Nevada Microearthquake Survey.* Report prepared for AMAX Exploration Inc. 8 October 1979.

MICROGEOPHYSICS CORP. (1980). *Self-potential Survey, McCoy, Nevada.* Report prepared for AMAX Exploration Inc. 15 June 1979.

TERRAPHYSICS (1980). *Telluric-Magnetotelluric Survey at McCoy Prospect, Churchill County, Nevada.* Report prepared for AMAX Exploration Inc. March 1980.

# THE McCOY, NEVADA GEOTHERMAL PROSPECT

*An Interim Case History*

PART II (Figures)

by Arthur L. Lange

*Paper delivered at the Fifieth Annual Meeting of the Society of Exploration Geophysicists, Houston, Texas, 17 November 1980.*

AMAX Exploration Inc.
Geothermal Branch
7100 W. 44th Avenue
Wheat Ridge, Colorado 80033

## FIGURES

1L. Location of the McCoy prospect.

2R. Orientation map, showing principal features of the McCoy prospect.

3L. View northward from McCoy Peak.

4L. The McCoy mercury mine.

5R Partial Landsat image showing the ring in center surrounding the McCoy prospect. Hole in the Wall wash drains the ring and empties into Dixie Valley on the west.

6L. Simplified geologic map, showing locations of McCoy and Wildhorse mines. PP, Permo-Pennsylvanian sediments; TRJ, Triassic-Jurassic conglomerates, carbonates and sandstones; T, Tertiary volcanics; Qal, Quaternary alluvium; Qt, Quaternary hot spring travertines. (after Pilkington, 1979).

7R. East-west geologic profile through McCoy mine (See Slide 9L), with profile of temperature @ 100m and conductive isotherms.

8L. Heatflow map showing thermal anomaly shaded, highest heatflows stippled and lowest, striped.

9L. Map of temperature at 100m showing thermal anomaly shaded, highest temperatures stippled, and lowest, striped.

10R. Profile of temperatures and isotherms along Line A (N/S).

11R. Profile of temperatures and isotherms with geologic section along Line C (E/W) (Geology after Pilkington, 1979).

12L. Isothermal section at Red Hill Hot Spring, Utah, from Chapman, Kilty & Mase, 1978. Compare with Line C isotherms.

13L. Complete Bouguer gravity map. Highs are stippled; lows, striped.

14R. Gravity profile, Line B, with automatic interpretation for densities 2.1 (checked) and 2.8gm/cm$^3$ (striped).

15R. Gravity profile, Line C, with automatic interpretation for densities 2.1 (checked) and 2.8gm/cm$^3$ (striped).

16L. Residual aeromagnetic map. Highs are stippled; lows, striped.

17R. Map of P-wave delays from teleseisms. Largest delays are striped; advances, stippled.

18L. Map of Poisson's Ratios (highs, striped; lows, stippled) showing also locations of microearthquake foci and fault-plane solutions.

19R. Profiles of P-wave delays and advances and Poisson's ratios along Line B.

20R. Profiles of P-wave delays and advances and Poisson's ratios along Line C.

21R. Profiles of P-wave delays and advances and Poisson's ratios along Line A.

22L. Map of self-potential response. Negatives are striped; highs stippled.

23R. Refer to Figure 9L.

24R. Self-potential profile, Line B, compared with profile of temperature at 100m and isotherms. Microearthquake epicenters shown as stars.

25R. Self-potential profile, Line A, compared with profile of temperature at 100m and isotherms. Microearthquake epicenters shown as stars.

26R. Self-potential profile, Line C, compared with profile of temperature at 100m and isotherms. Microearthquake epicenters shown as stars.

27L. Resistivity at 5km depth from 1D magnetotelluric inversion ($T_e$ mode). Conductive zones stippled; resistive striped.

28R. Magnetotelluric section ($T_e$ mode, 1D inversion) along Line B compared with available EM section and geology.

29R. MT section ($T_e$ mode, 1D inversion) along Line A compared with available EM data.

30R. MT pseudosections (resistivity vs. period) along Line C.

31R. MT section ($T_e$ mode, 1D inversion) along Line C, compared with geologic section.

32L. Refer to Figure 8L.

33R. Geologic section along Line C, showing deduced geothermal reservoir feeding conduit of ascending hot water along limb of horst block. Upon encountering the Triassic conglomerate, hot water (probably cooled by cold meteoric water from the surface) drains westward--downdip--to eventually return to the deep system.

## PLATES

Plate I. Stacked profiles of Line A.

Plate II. Stacked profiles of Line B.

Plate III. Stacked profiles of Line C.

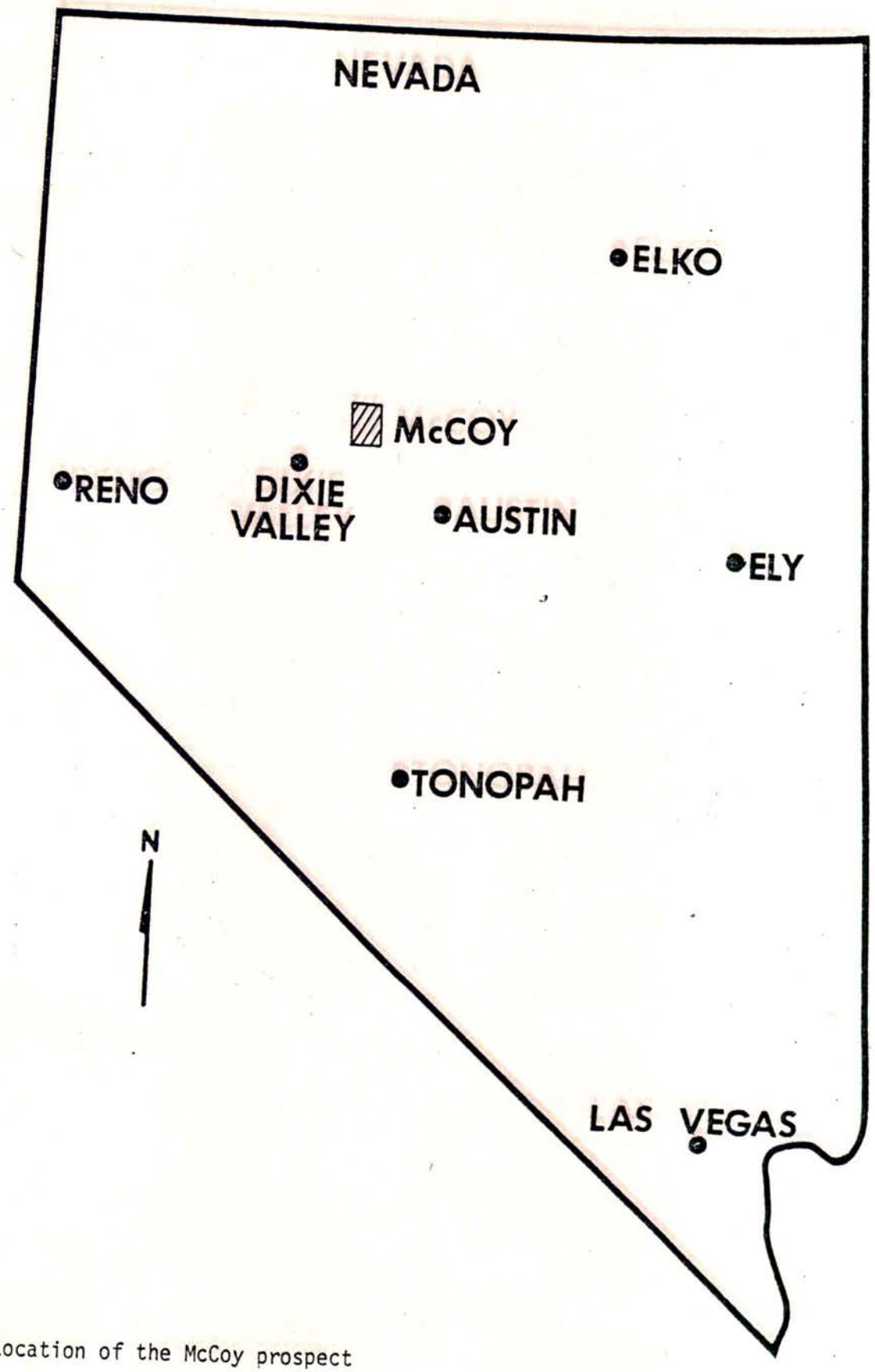


1L. Location of the McCoy prospect

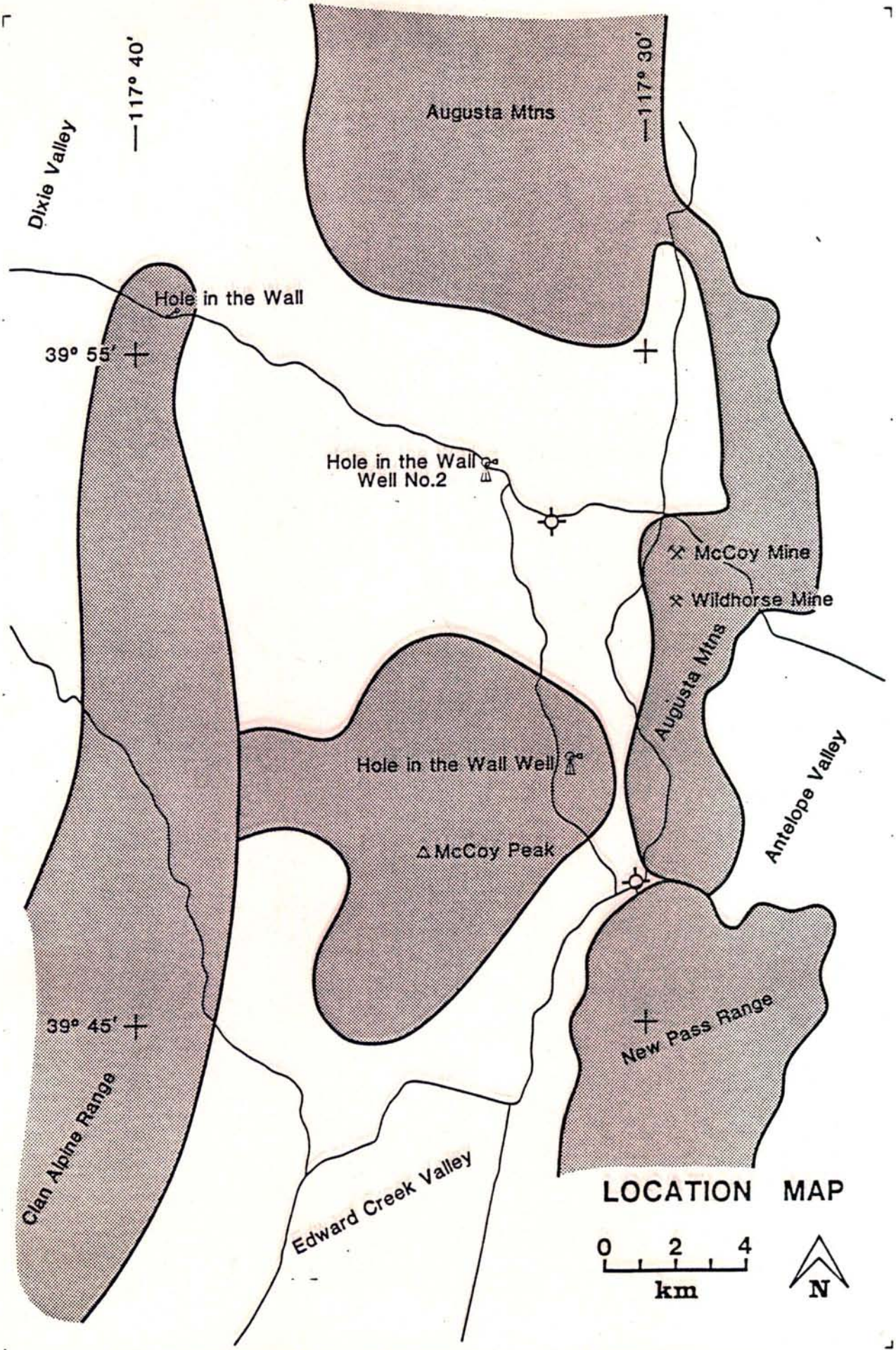


2R. Orientation map, showing principal features of the McCoy prospect

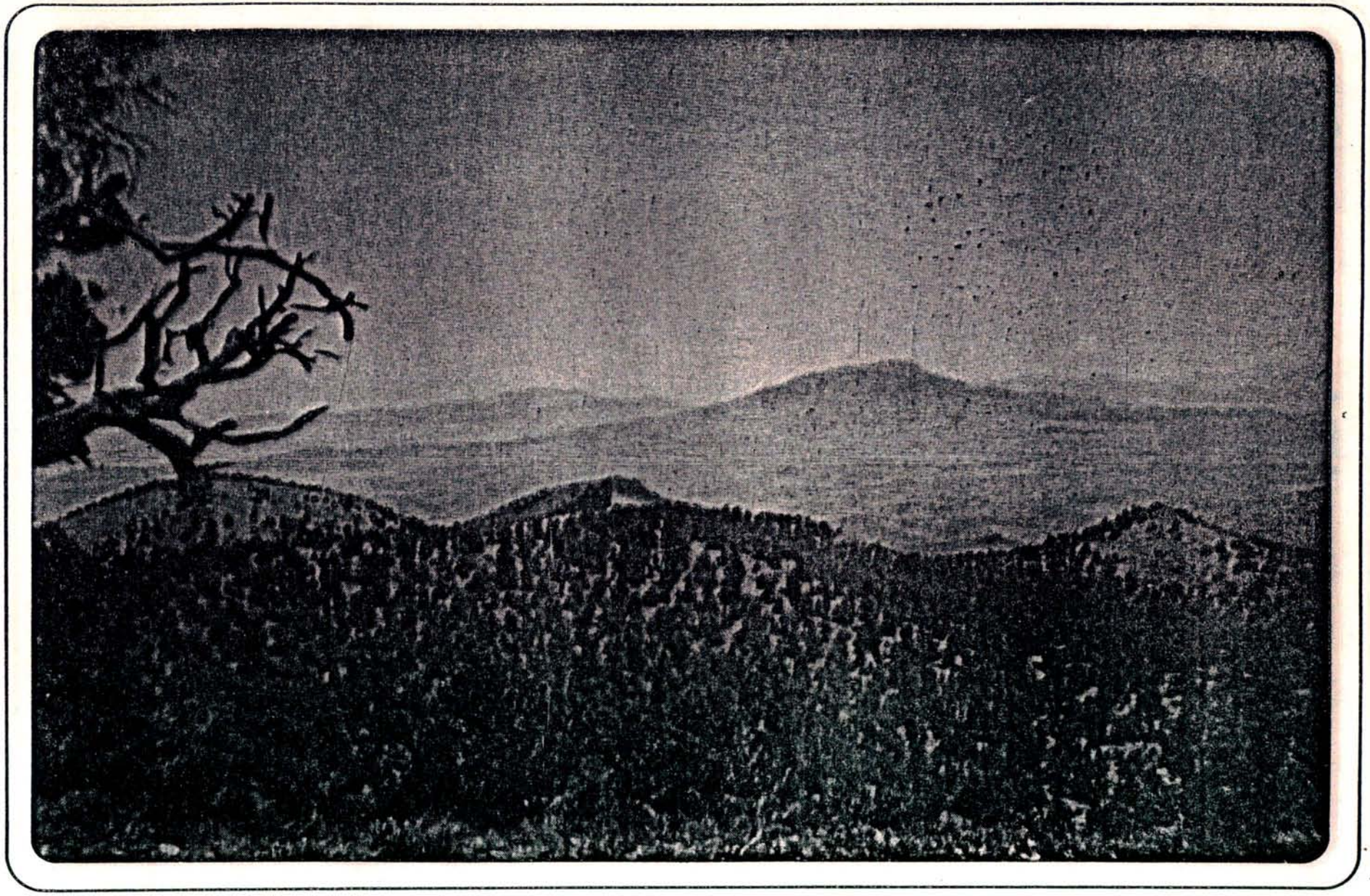

3L. View northward from McCoy Peak

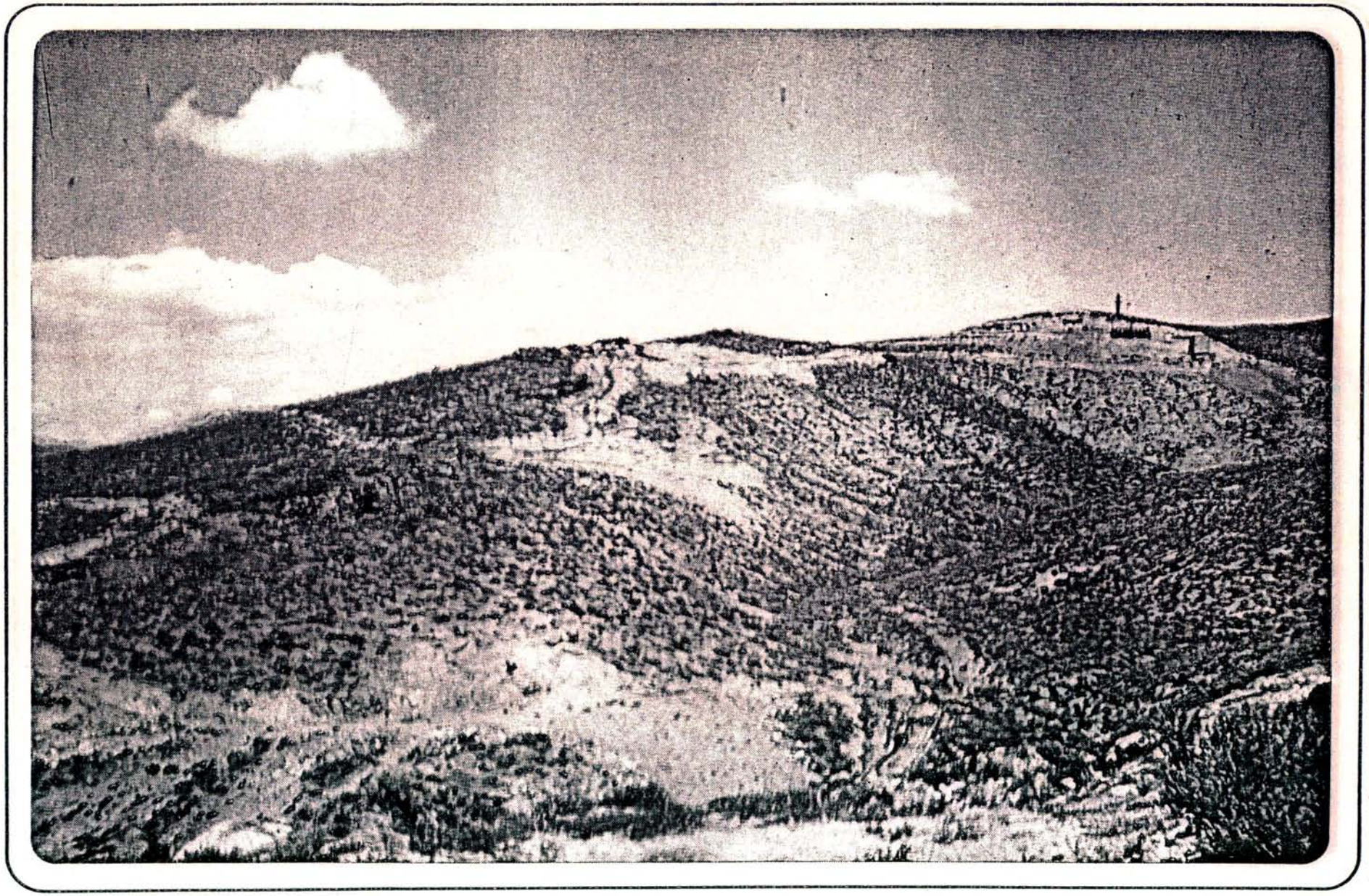

4L. The McCoy mercury mine

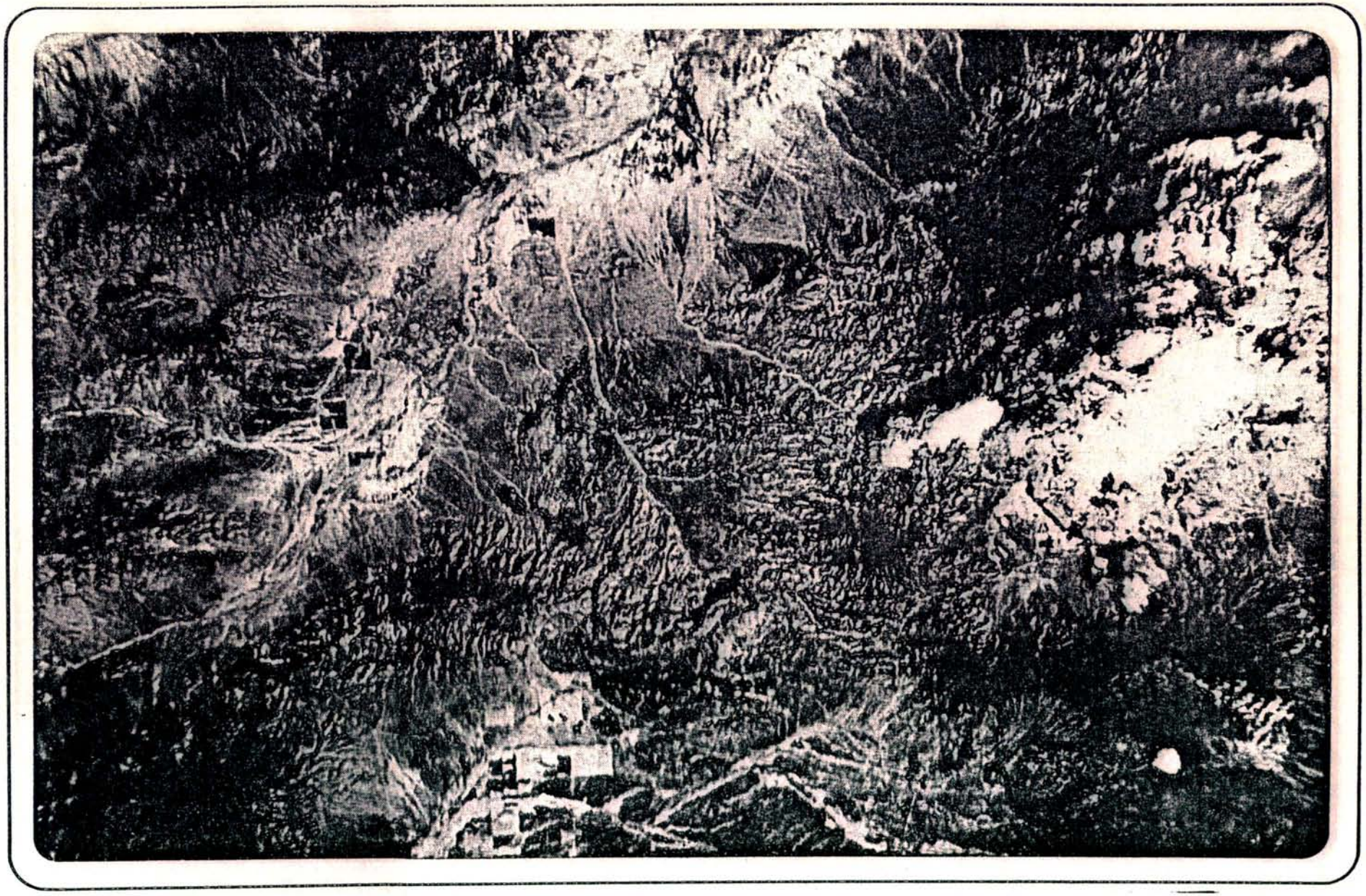

5R. Partial Landsat image showing the ring in center surrounding the McCoy prospect. Hole in the Wall wash drains the ring and empties into Dixie Valley on the west

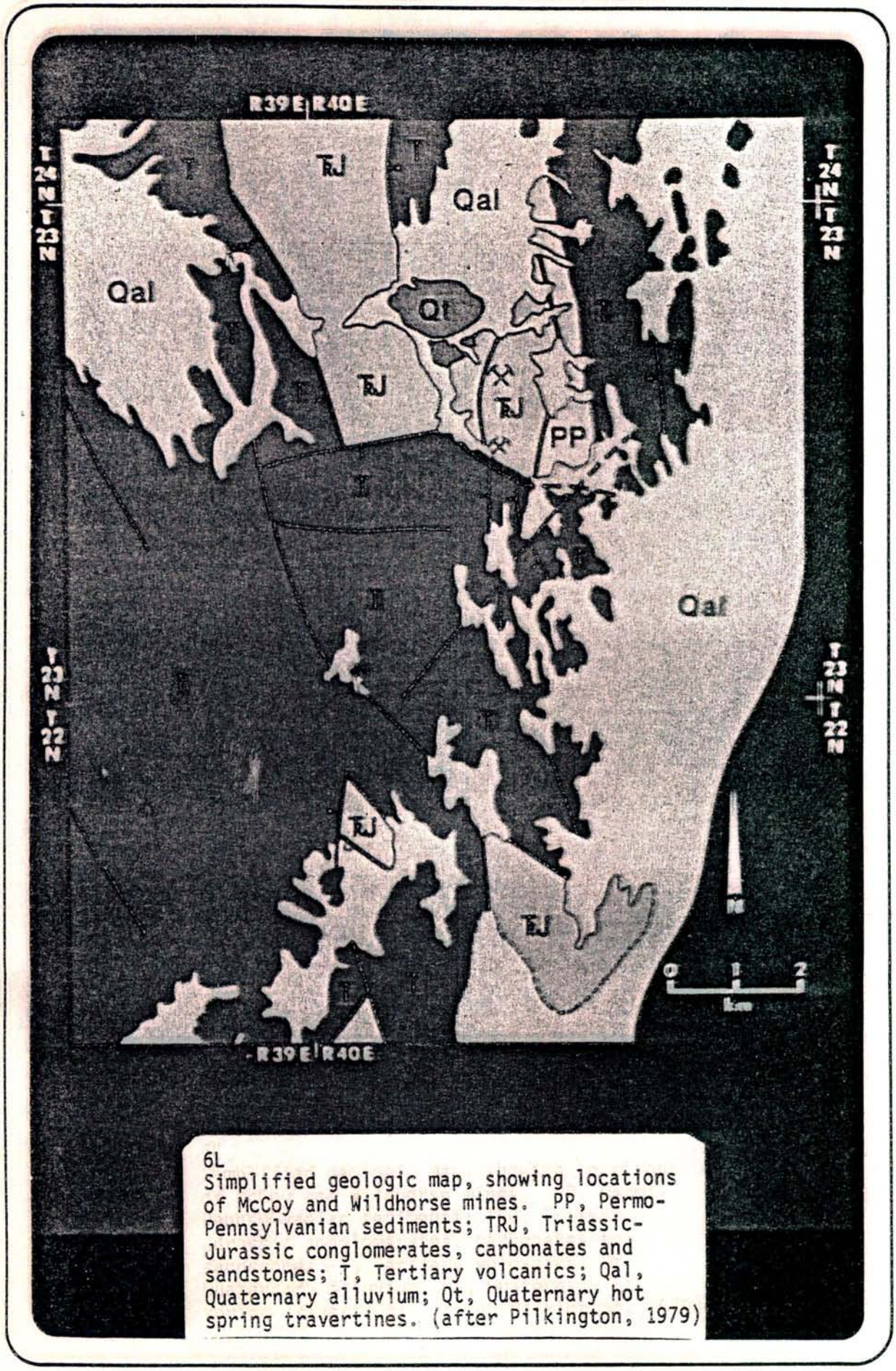


6L
Simplified geologic map, showing locations of McCoy and Wildhorse mines. PP, Permo-Pennsylvanian sediments; TRJ, Triassic-Jurassic conglomerates, carbonates and sandstones; T, Tertiary volcanics; Qal, Quaternary alluvium; Qt, Quaternary hot spring travertines. (after Pilkington, 1979)

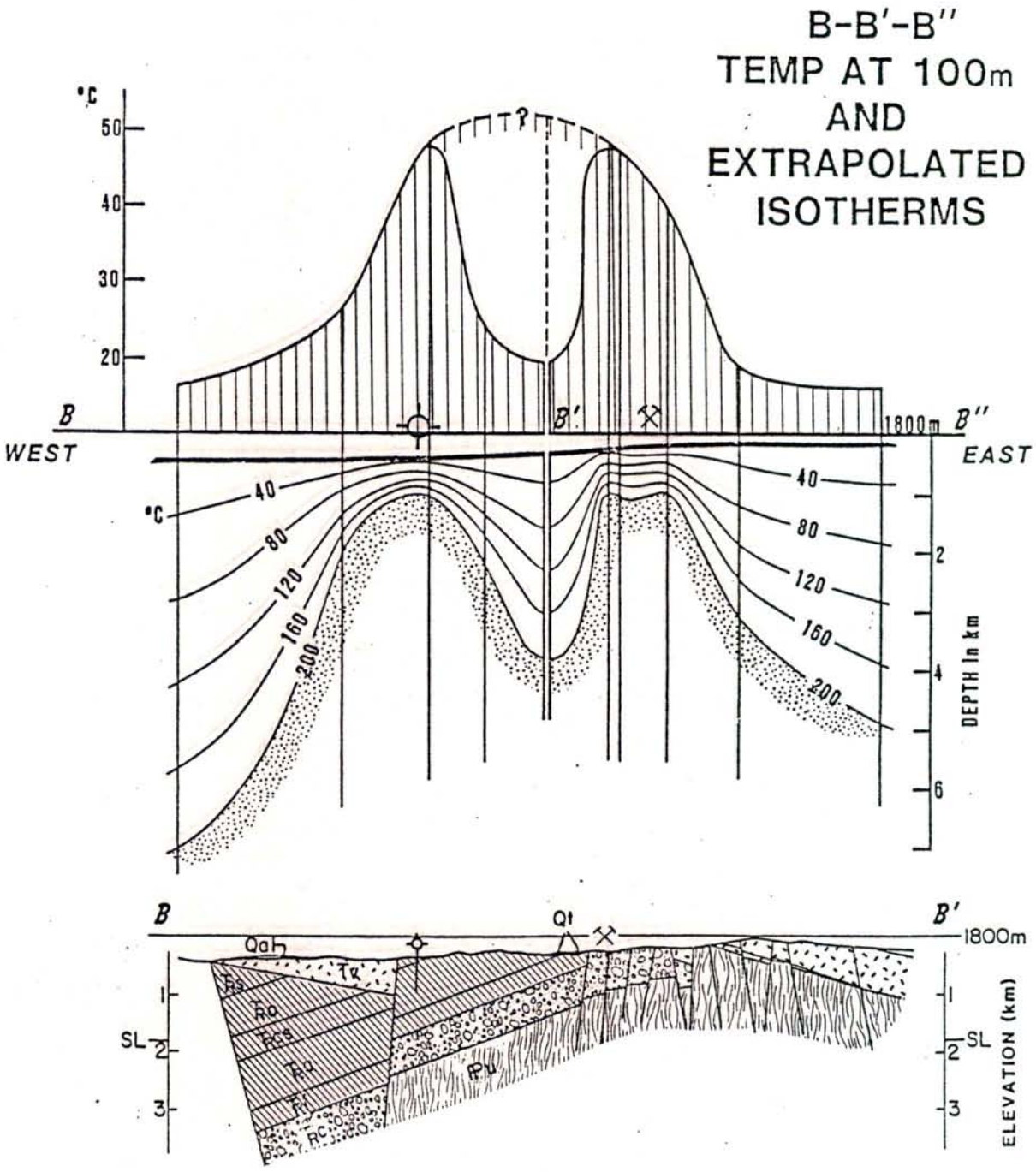


7R. East-west geologic profile through McCoy mine (See Slide 9L), with profile of temperature @ 100m and conductive isotherms

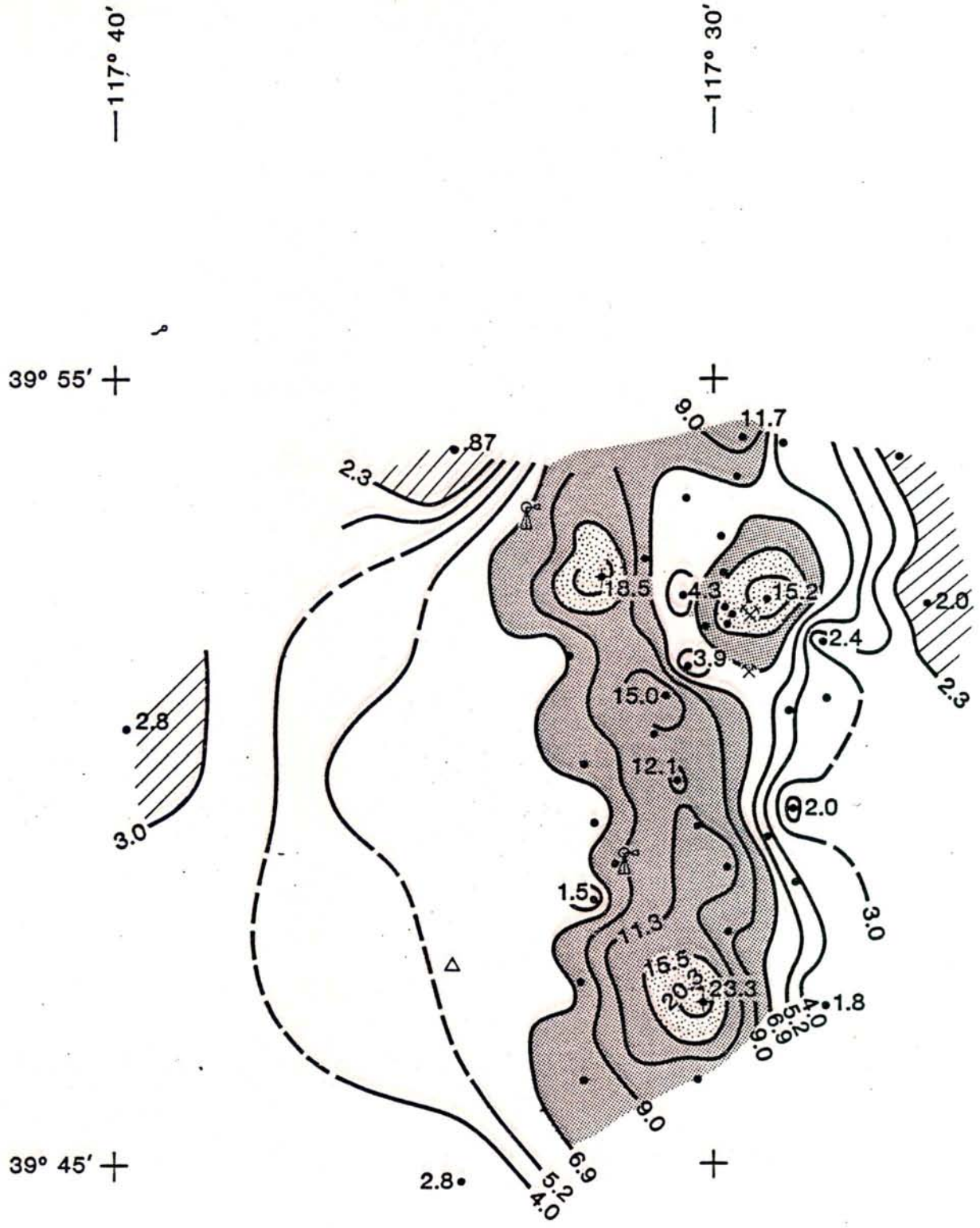


HEAT FLOW (HFU)

• WELLS

0 2 4

km

N

8L. Heatflow map showing thermal anomaly shaded, highest heatflows stippled and lowest, striped

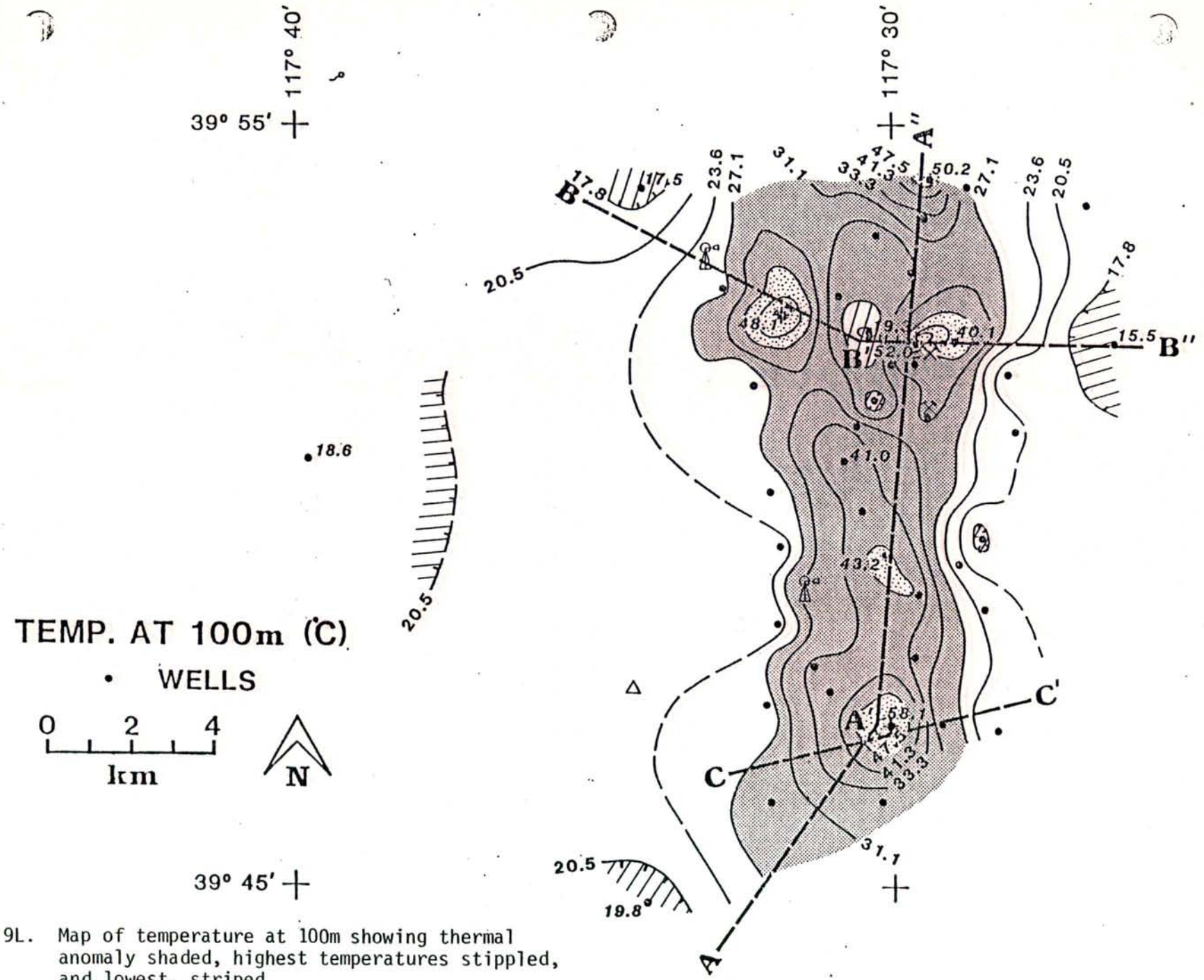


9L. Map of temperature at 100m showing thermal anomaly shaded, highest temperatures stippled, and lowest, striped

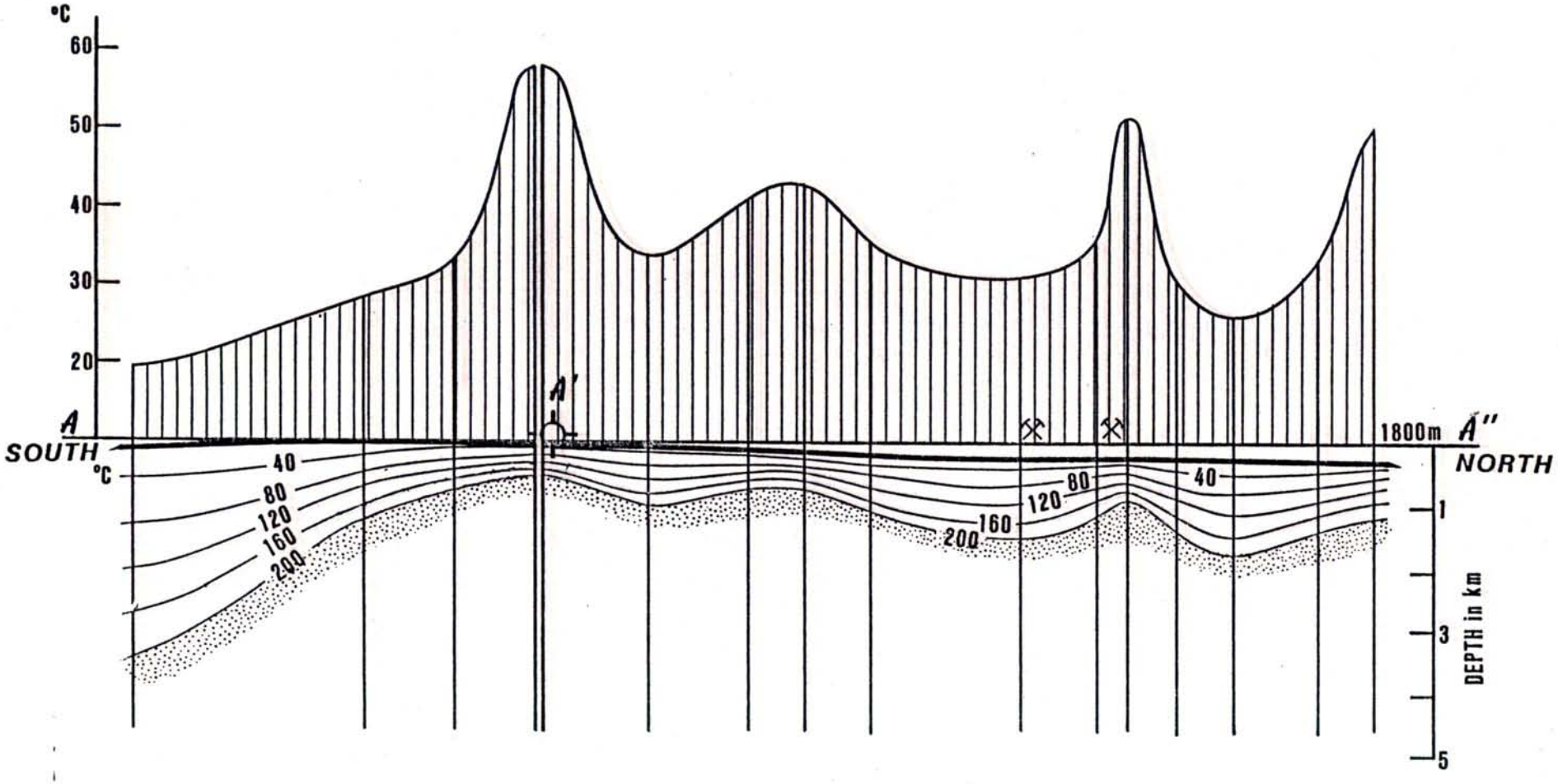


# TEMPERATURE AT 100m AND EXTRAPOLATED ISOTHERMS

10R. Profile of temperatures and isotherms along Line A (N/S)

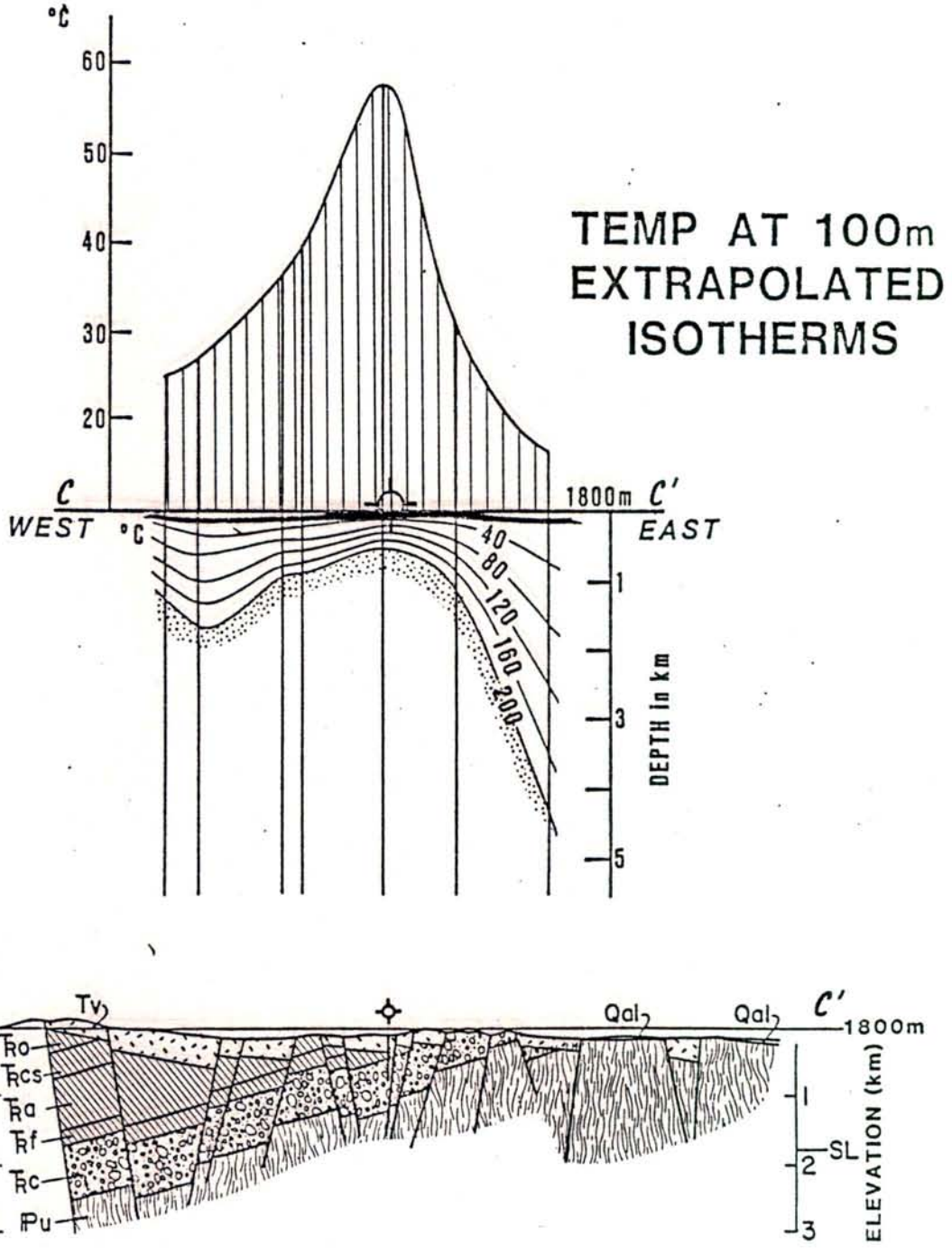


11R. Profile of temperatures and isotherms with geologic section along Line C (E/W) (Geology after Pilkington, 1979)

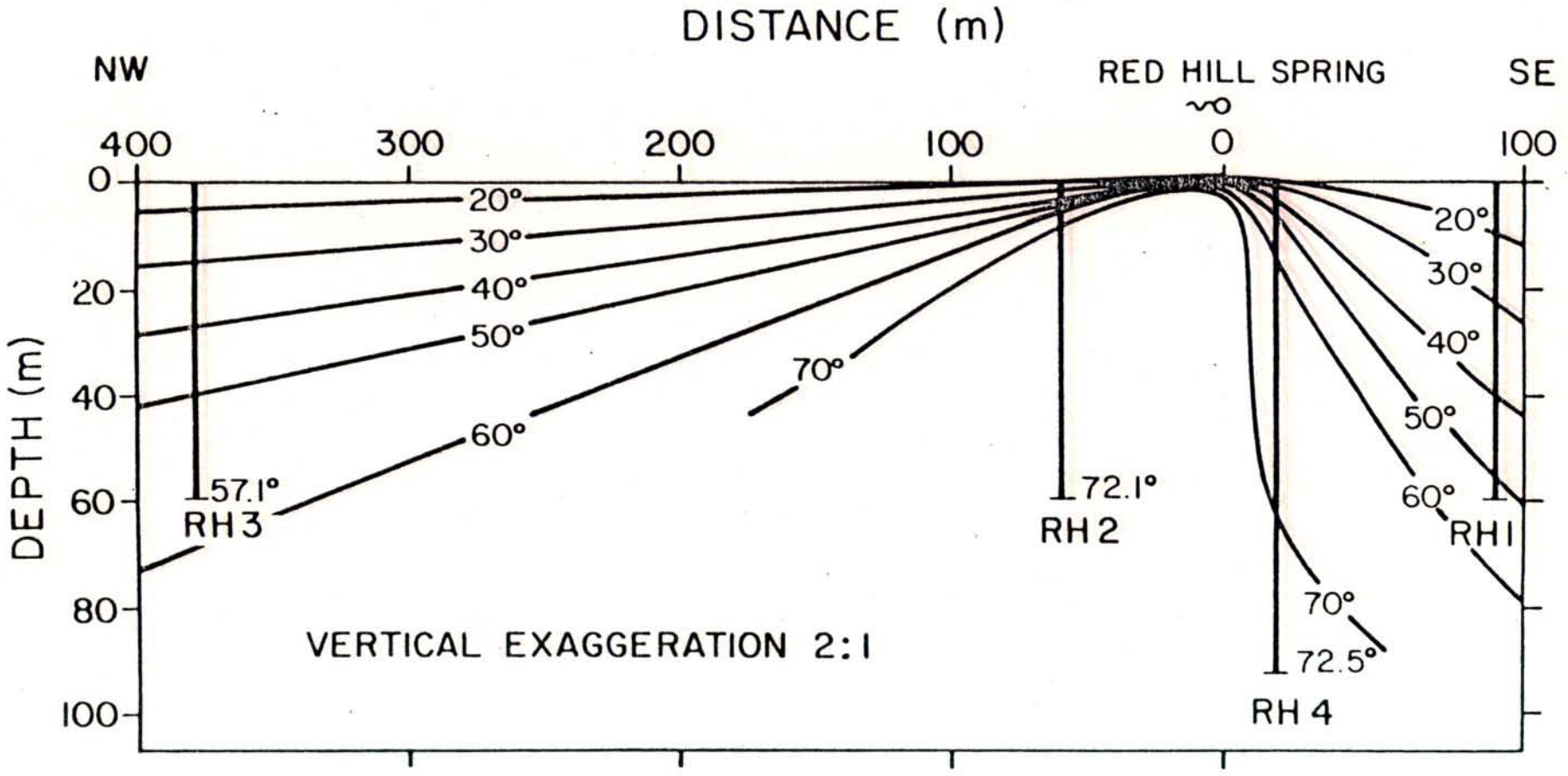


12L. Isothermal section at Red Hill Hot Spring, Utah, from Chapman, Kilty & Mase, 1978. Compare with Line C isotherms

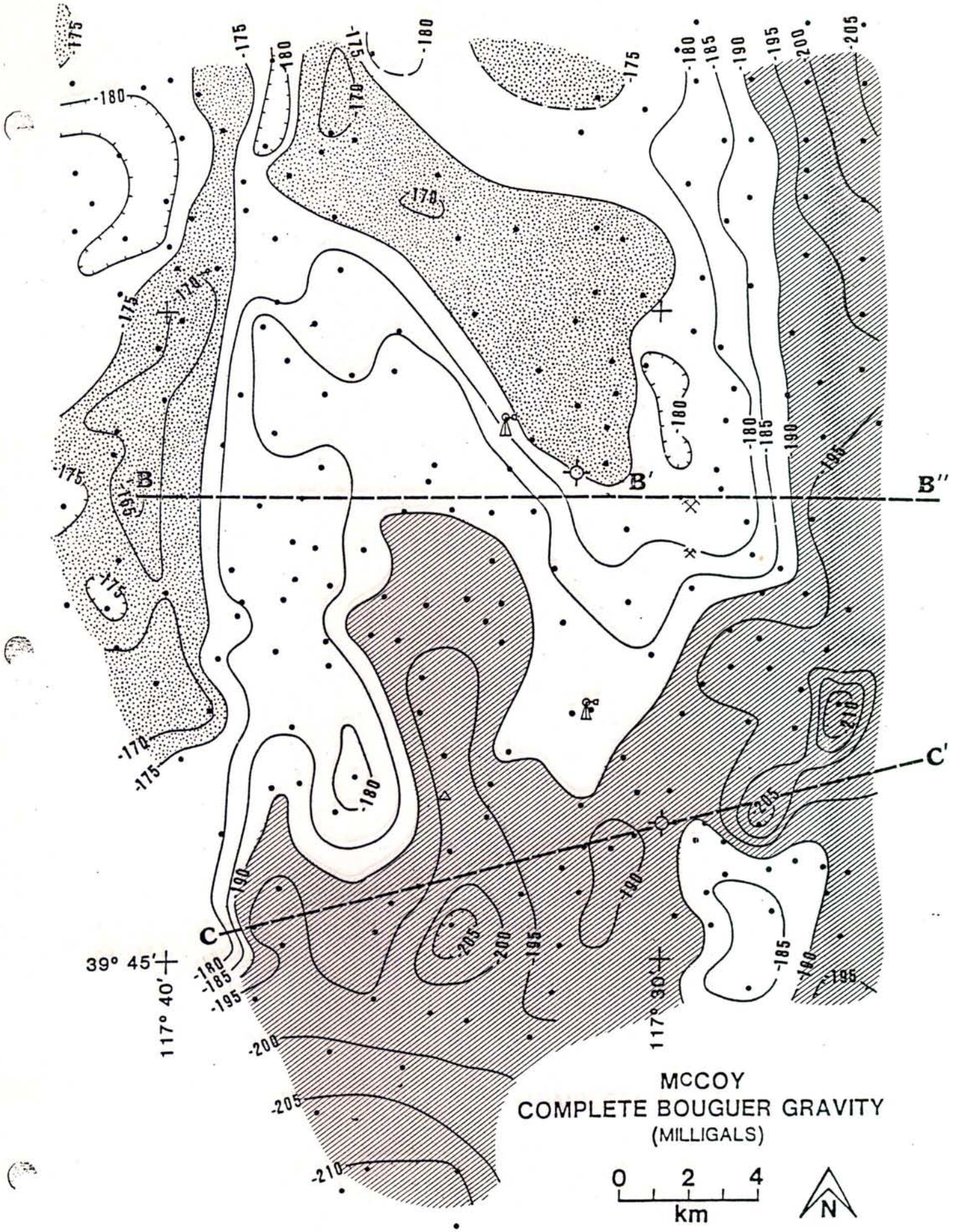


13L. Complete Bouguer gravity map. Highs are stippled; lows, striped

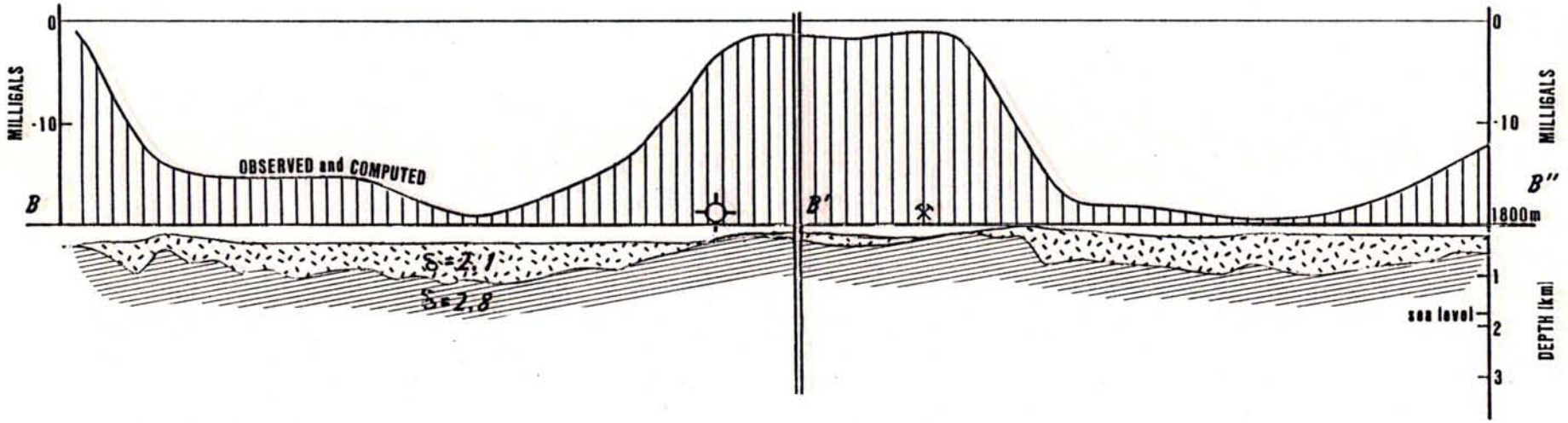


**B-B'-B''**
**RESIDUAL GRAVITY PROFILE (COMPLETE BOUGUER) AND DEPTH ANALYSIS**

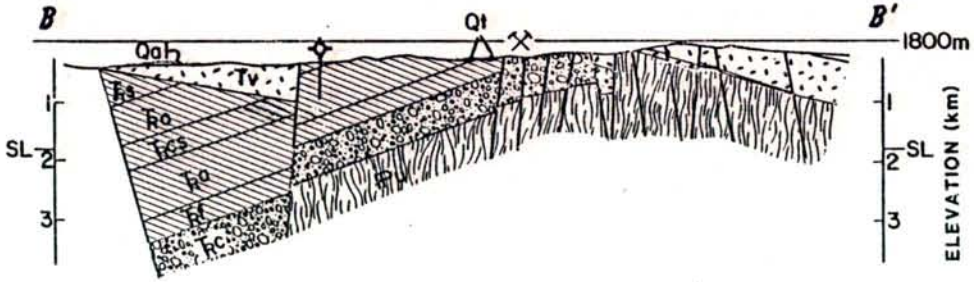


14R. Gravity profile, Line B, with automatic interpretation for densities 2.1 (checked) and 2.8gm/cm$^3$ (striped)

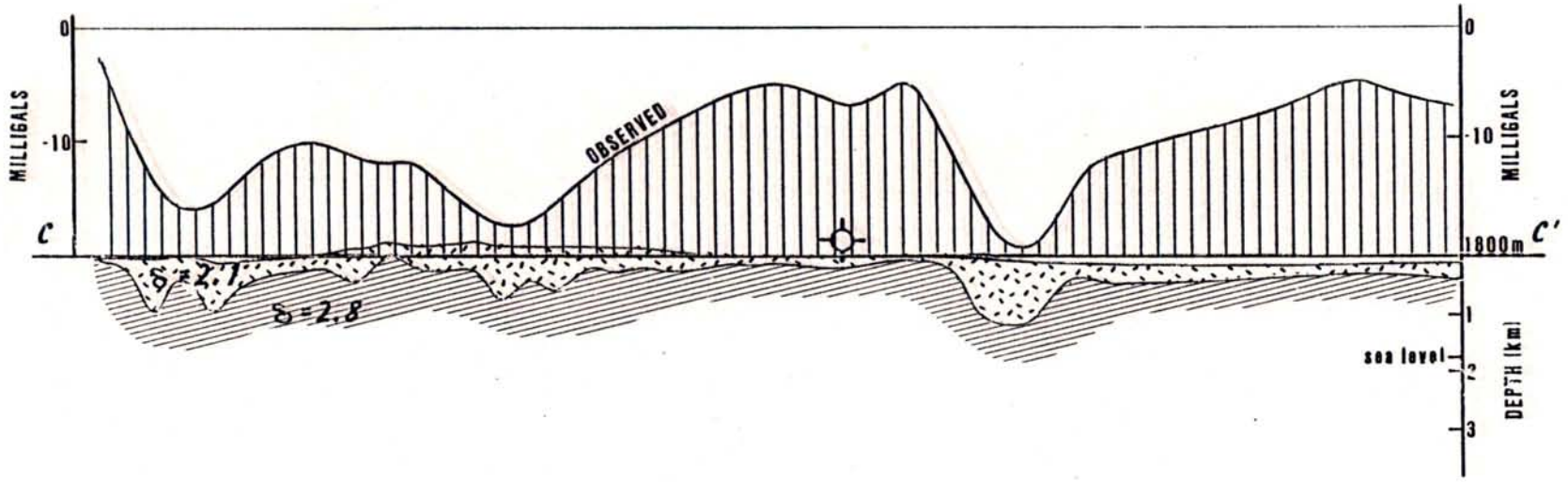


# C-C'
# RESIDUAL GRAVITY PROFILE (COMPLETE BOUGUER) AND DEPTH ANALYSIS

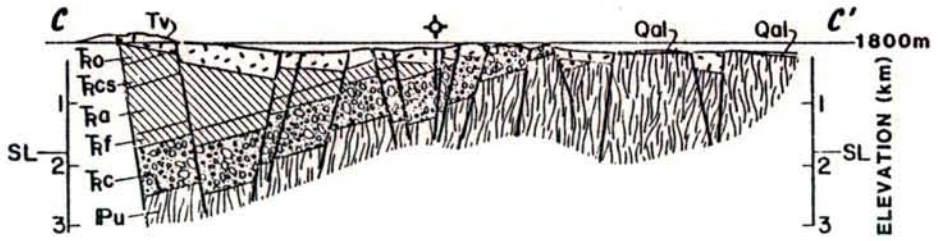


15R. Gravity profile, Line C, with automatic interpretation for densities 2.1 (checked) and 2.8gm/cm$^3$ (striped)

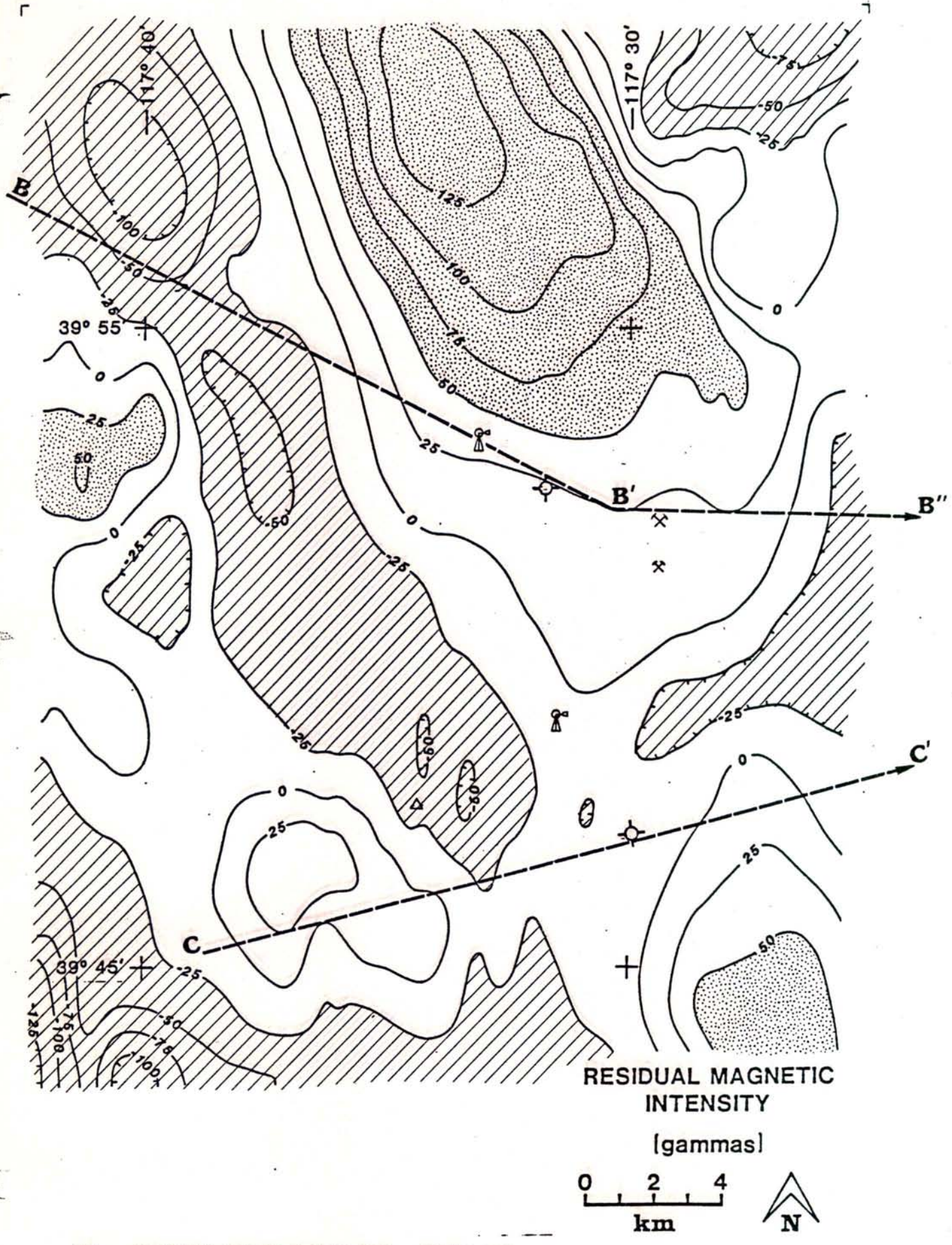


16L. Residual aeromagnetic map. Highs are stippled; lows, striped

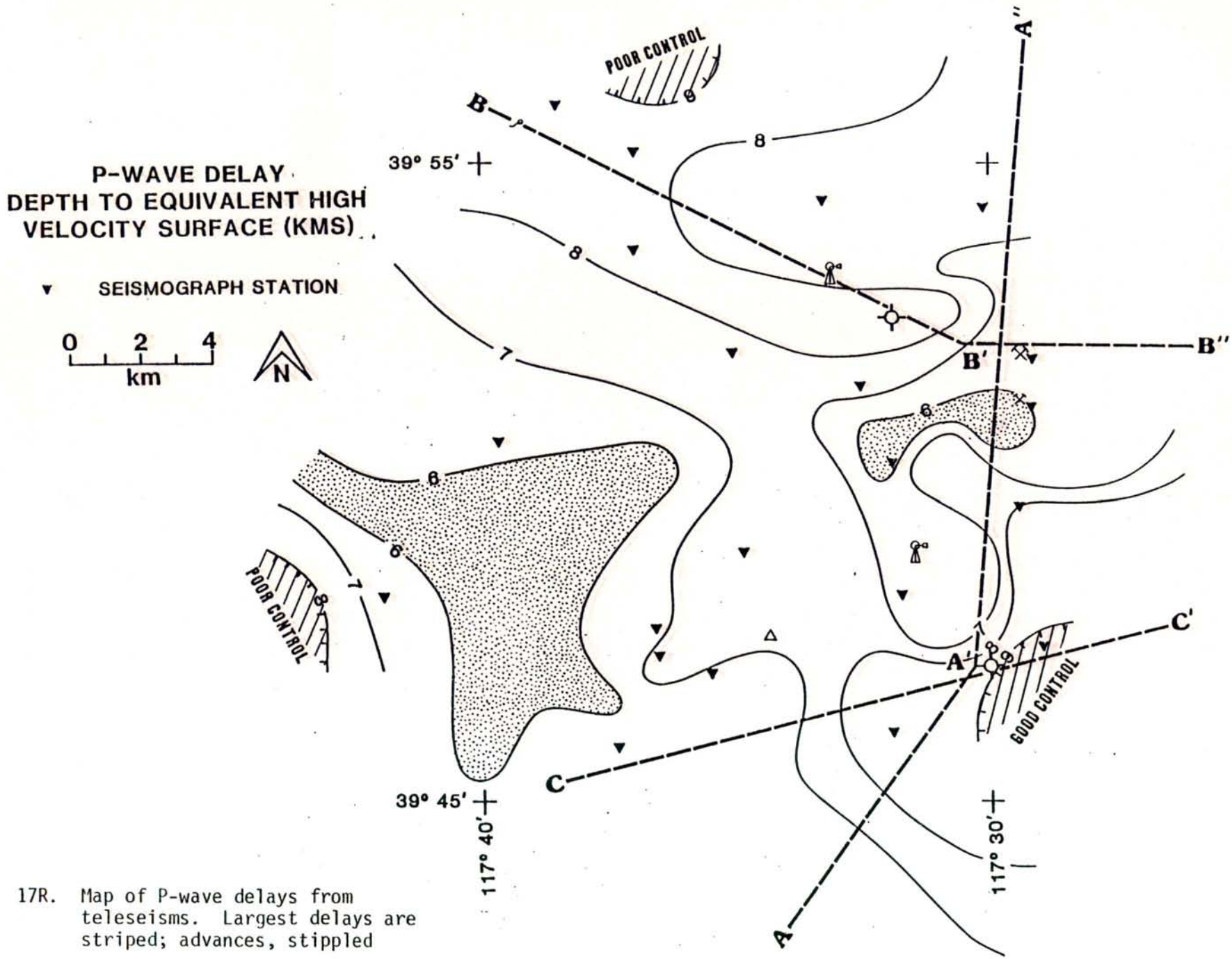


17R. Map of P-wave delays from teleseisms. Largest delays are striped; advances, stippled

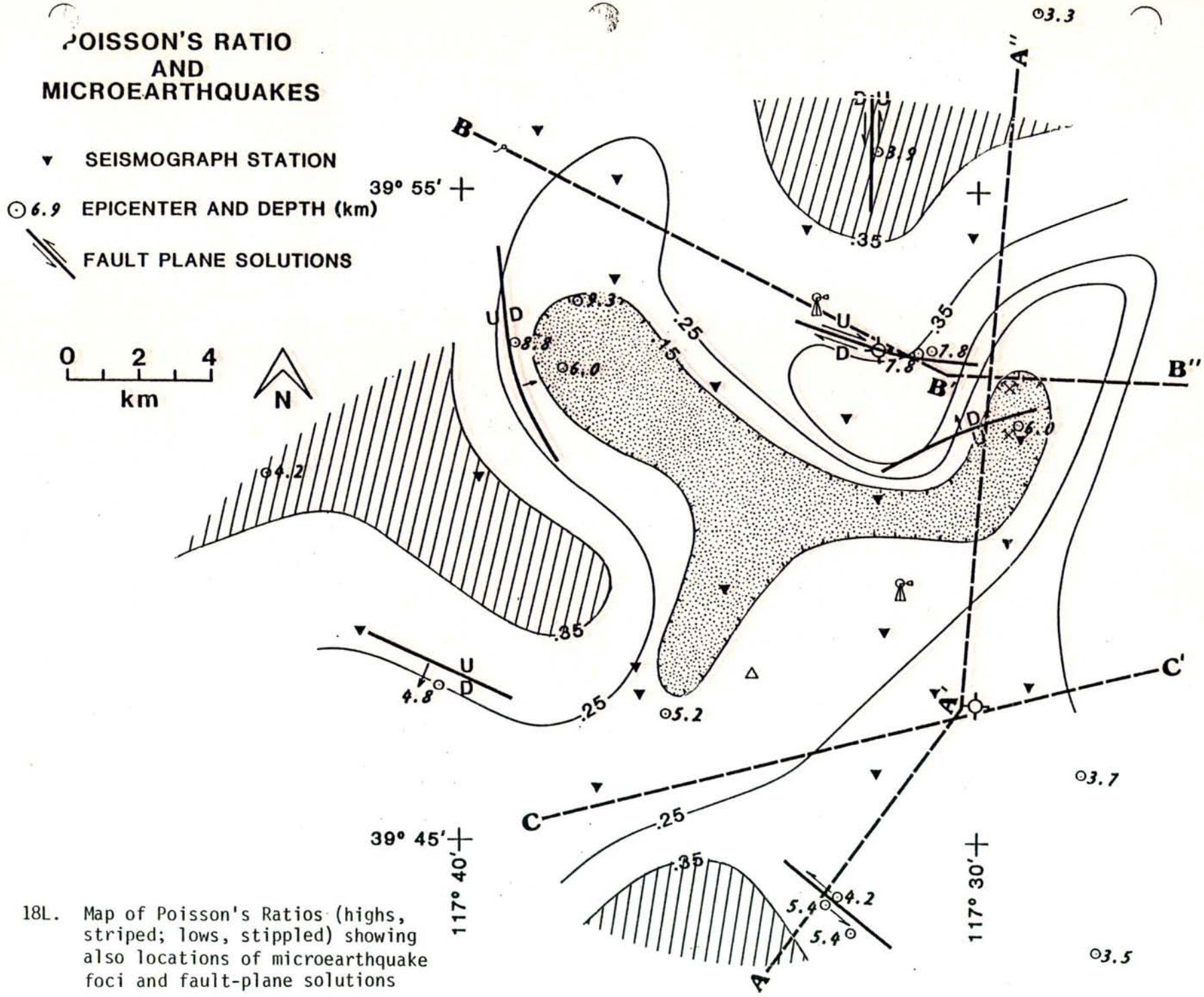


18L. Map of Poisson's Ratios (highs, striped; lows, stippled) showing also locations of microearthquake foci and fault-plane solutions

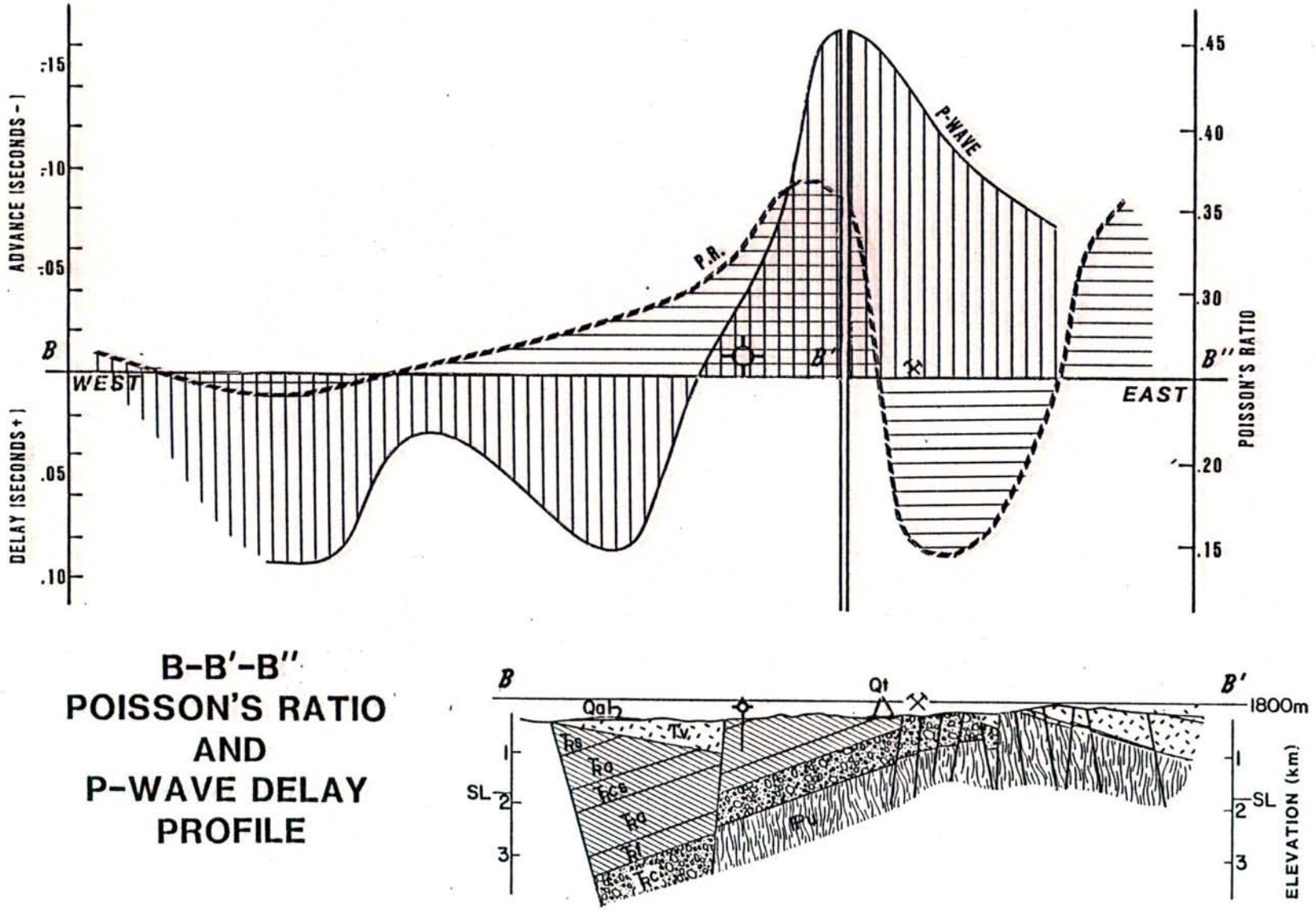


19R. Profiles of P-wave delays and advances and Poisson's Ratios along Line B

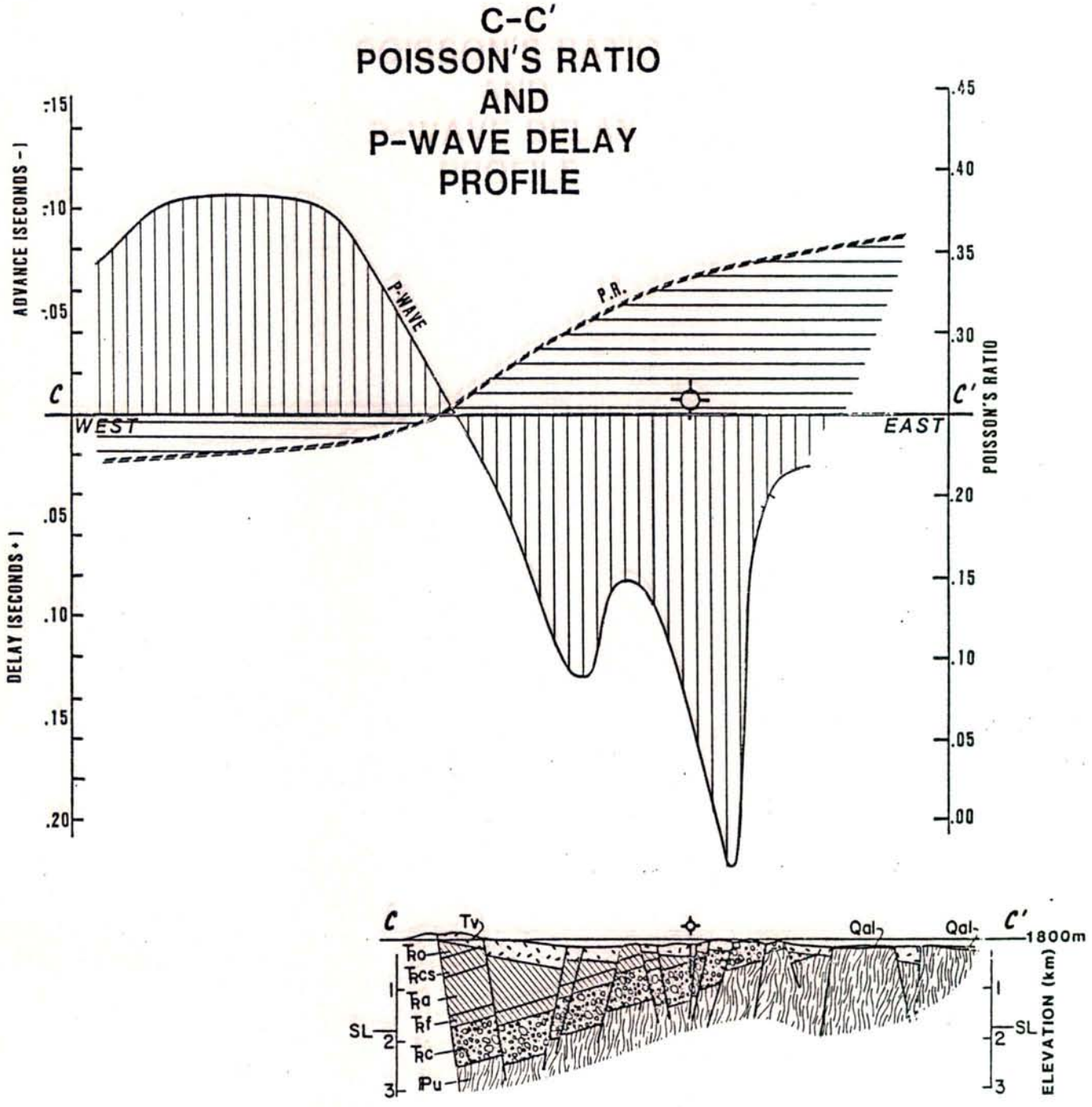


20R. Profiles of P-wave delays and advances and Poisson's Ratios along Line C

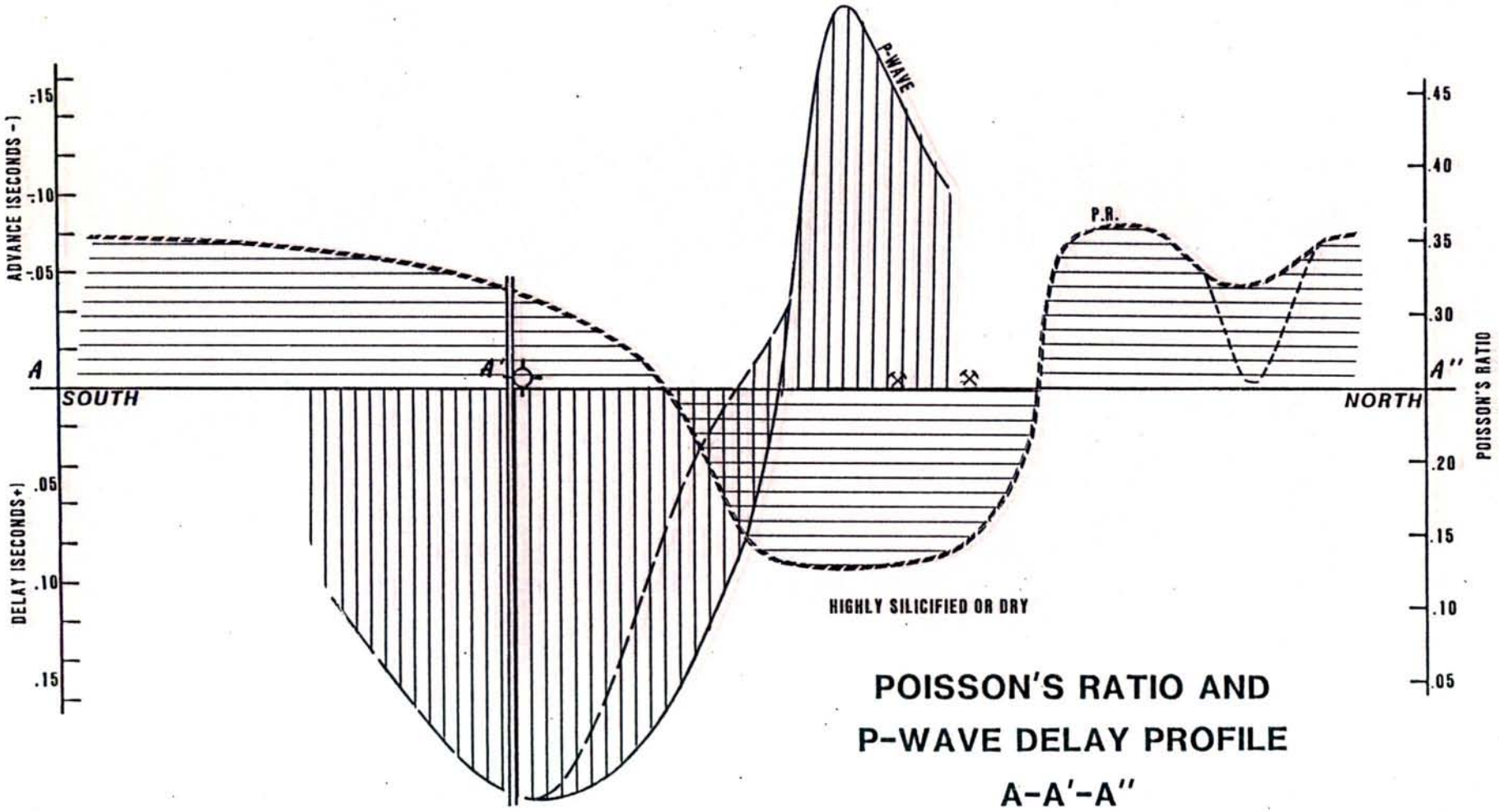


21R. Profiles of P-wave delays and advances and Poisson's Ratios along Line A

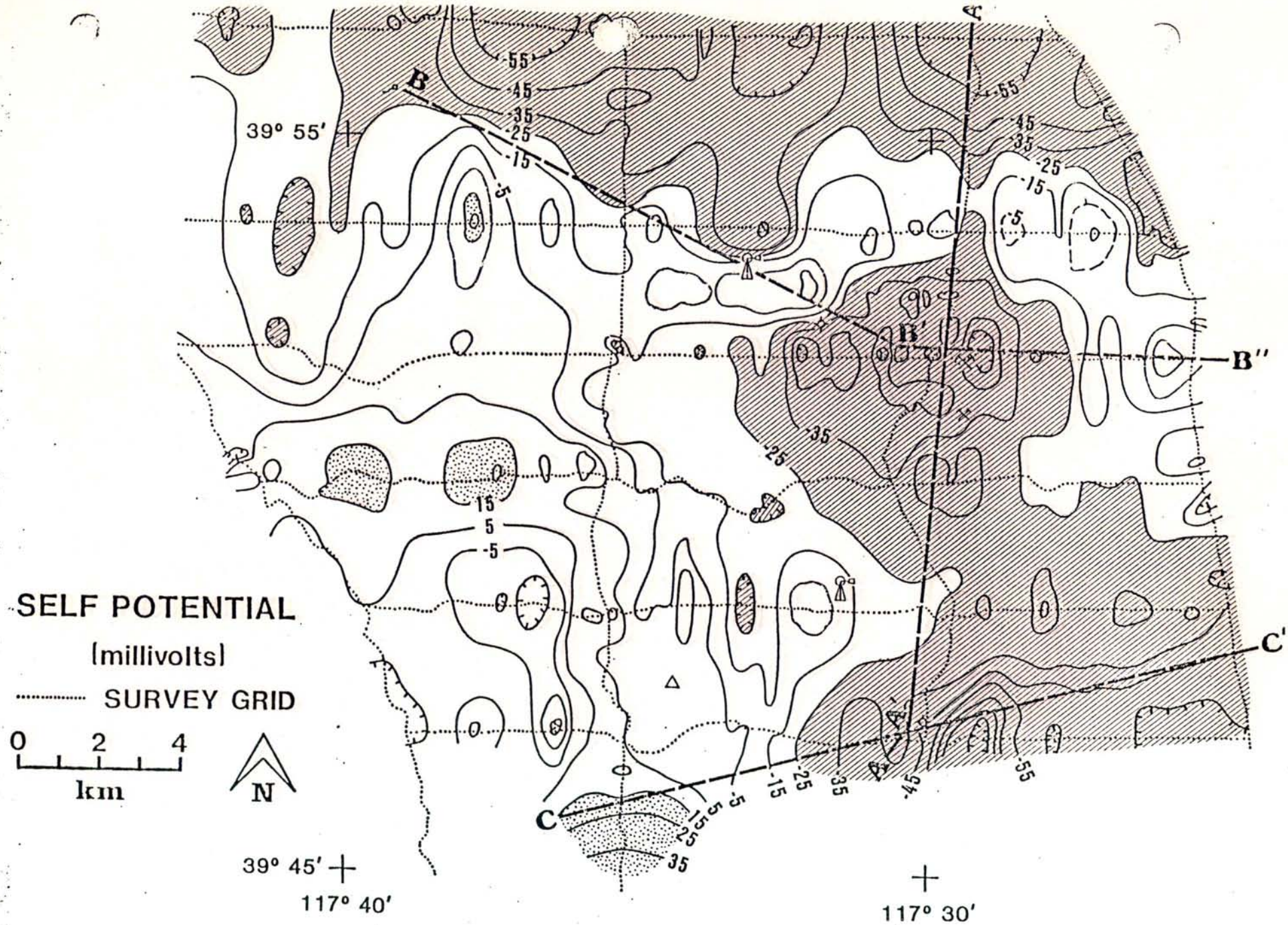


22L. Map of self-potential response. Negatives are striped; highs stippled

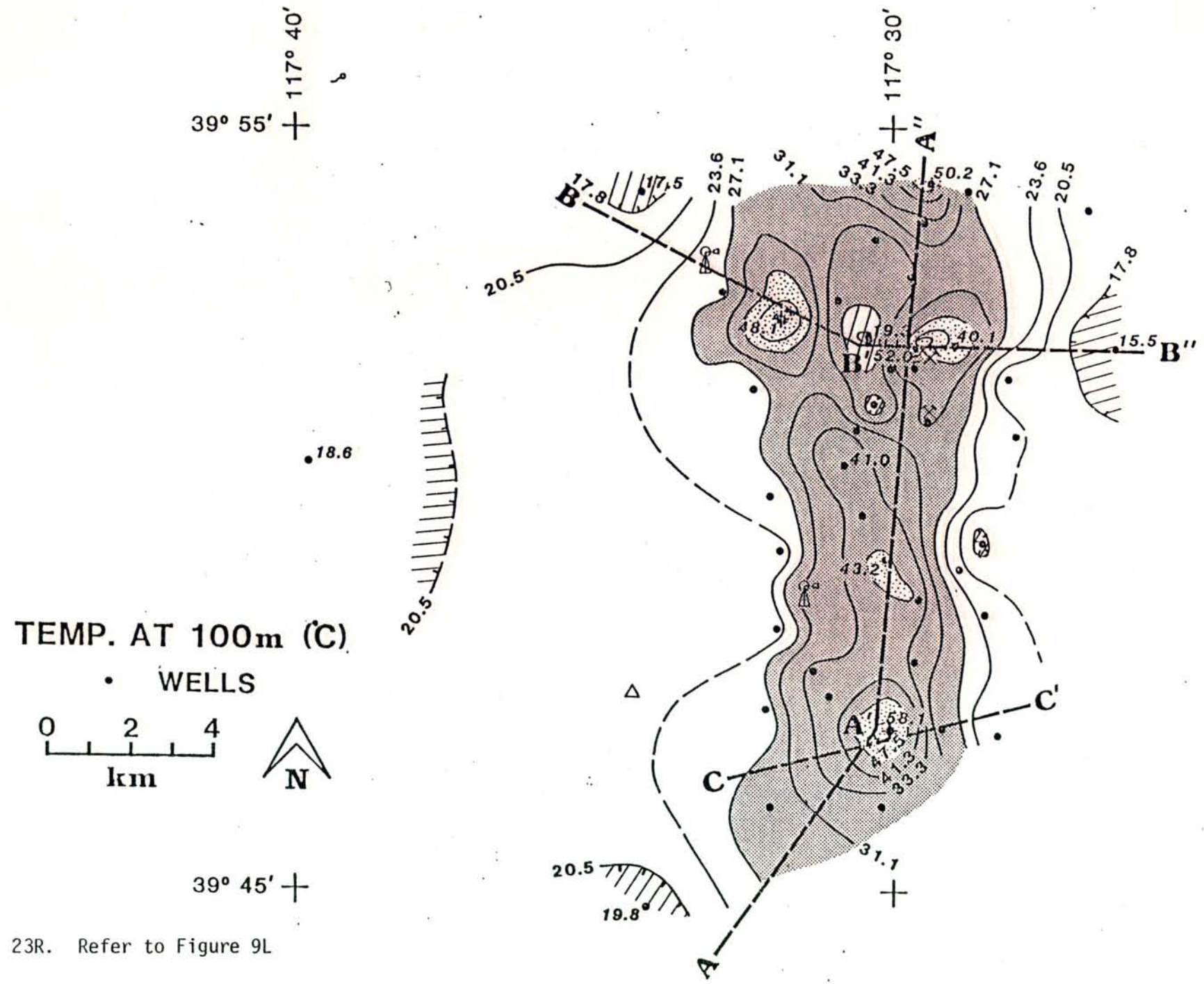


23R. Refer to Figure 9L

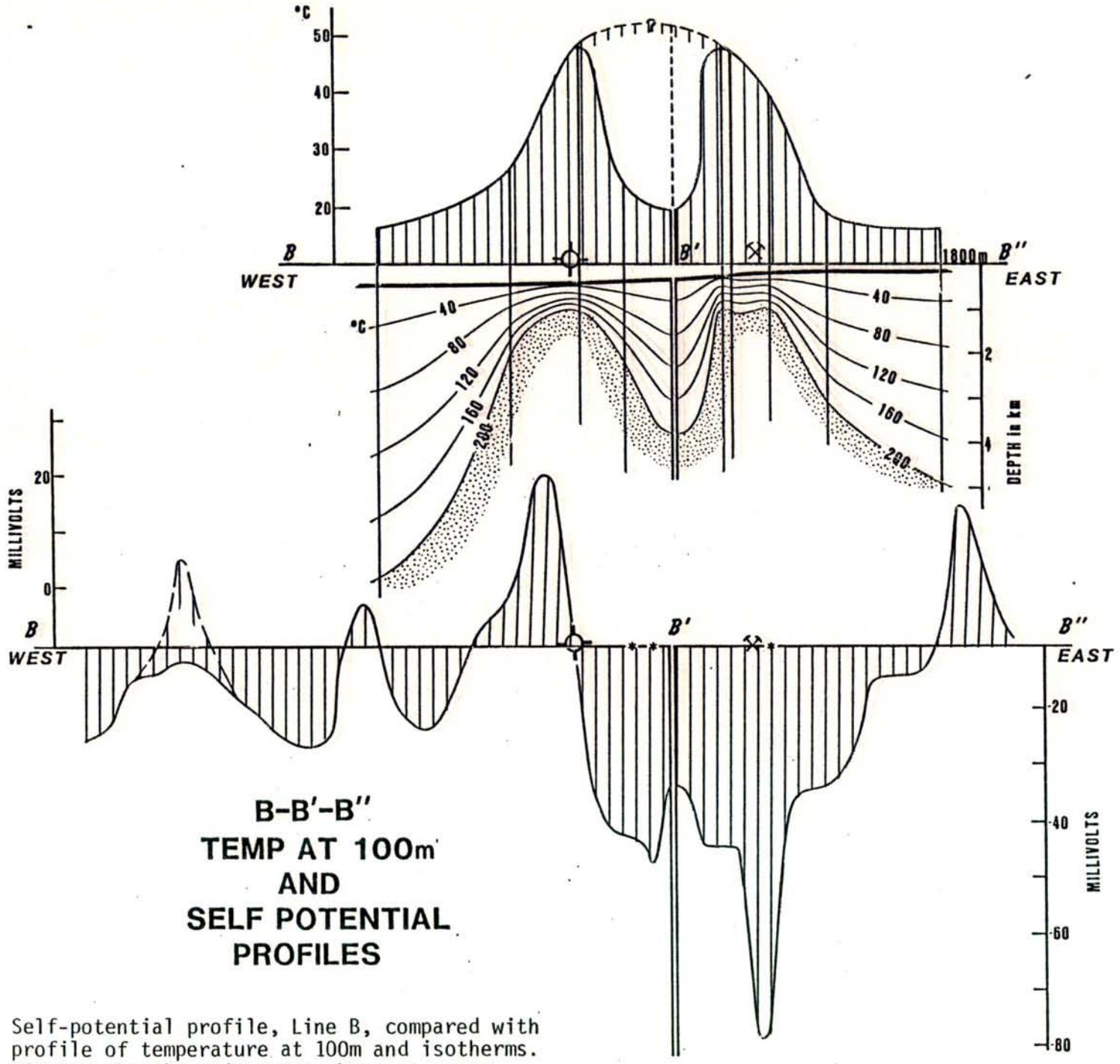


24R. Self-potential profile, Line B, compared with profile of temperature at 100m and isotherms. Microearthquake epicenters shown as stars

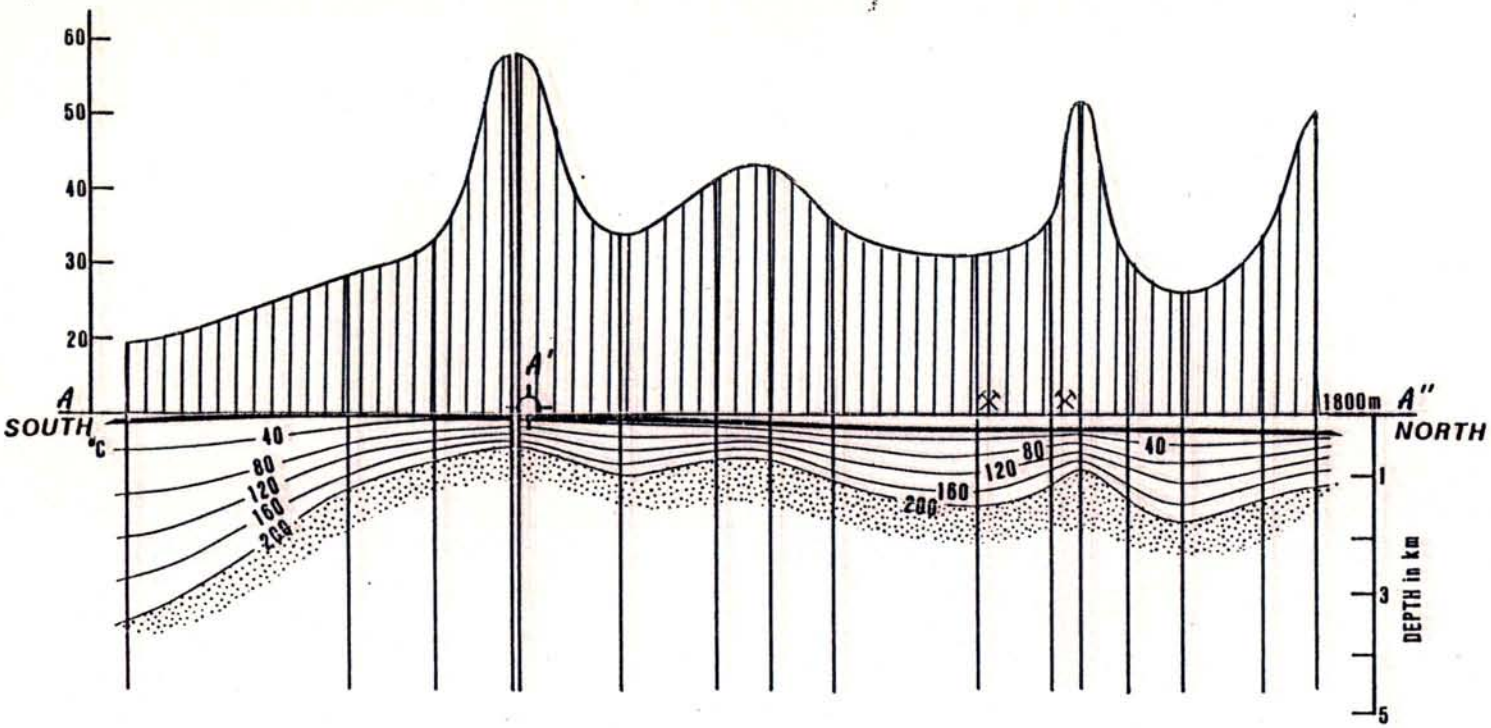


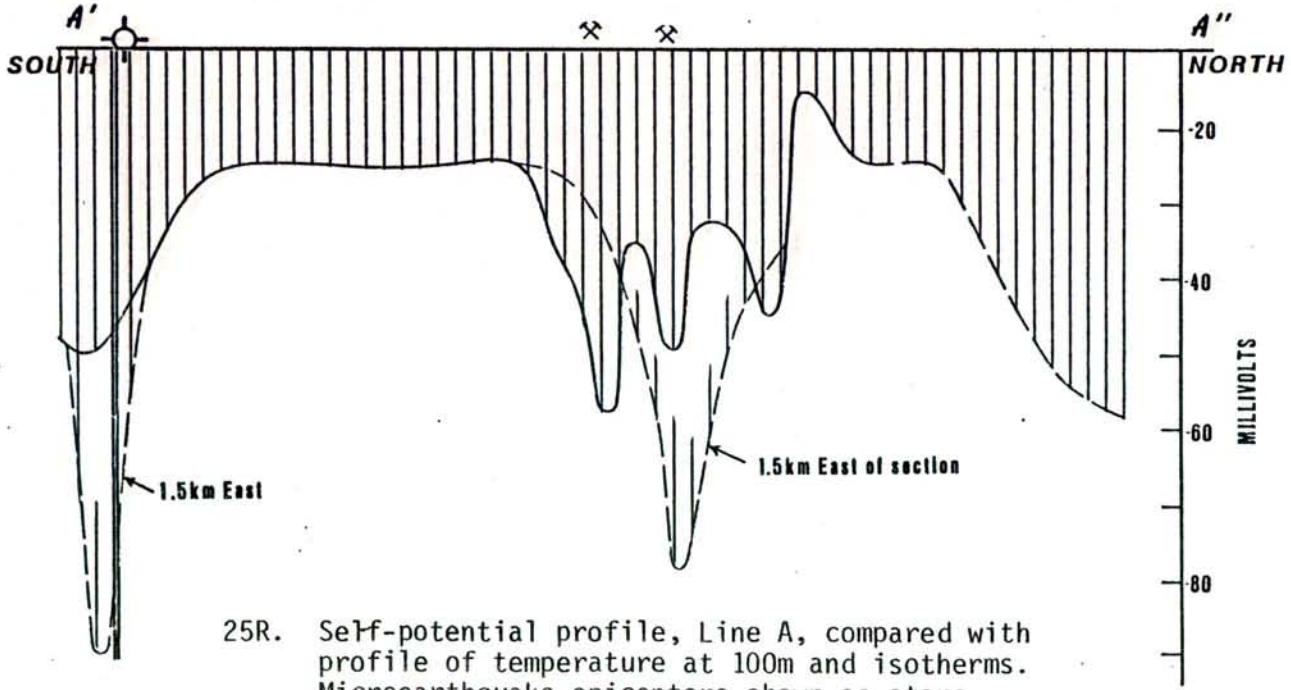


**A-A'-A"**
**TEMP AT 100m**
**AND**
**SELF POTENTIAL**
**PROFILES**

25R. Self-potential profile, Line A, compared with profile of temperature at 100m and isotherms. Microearthquake epicenters shown as stars

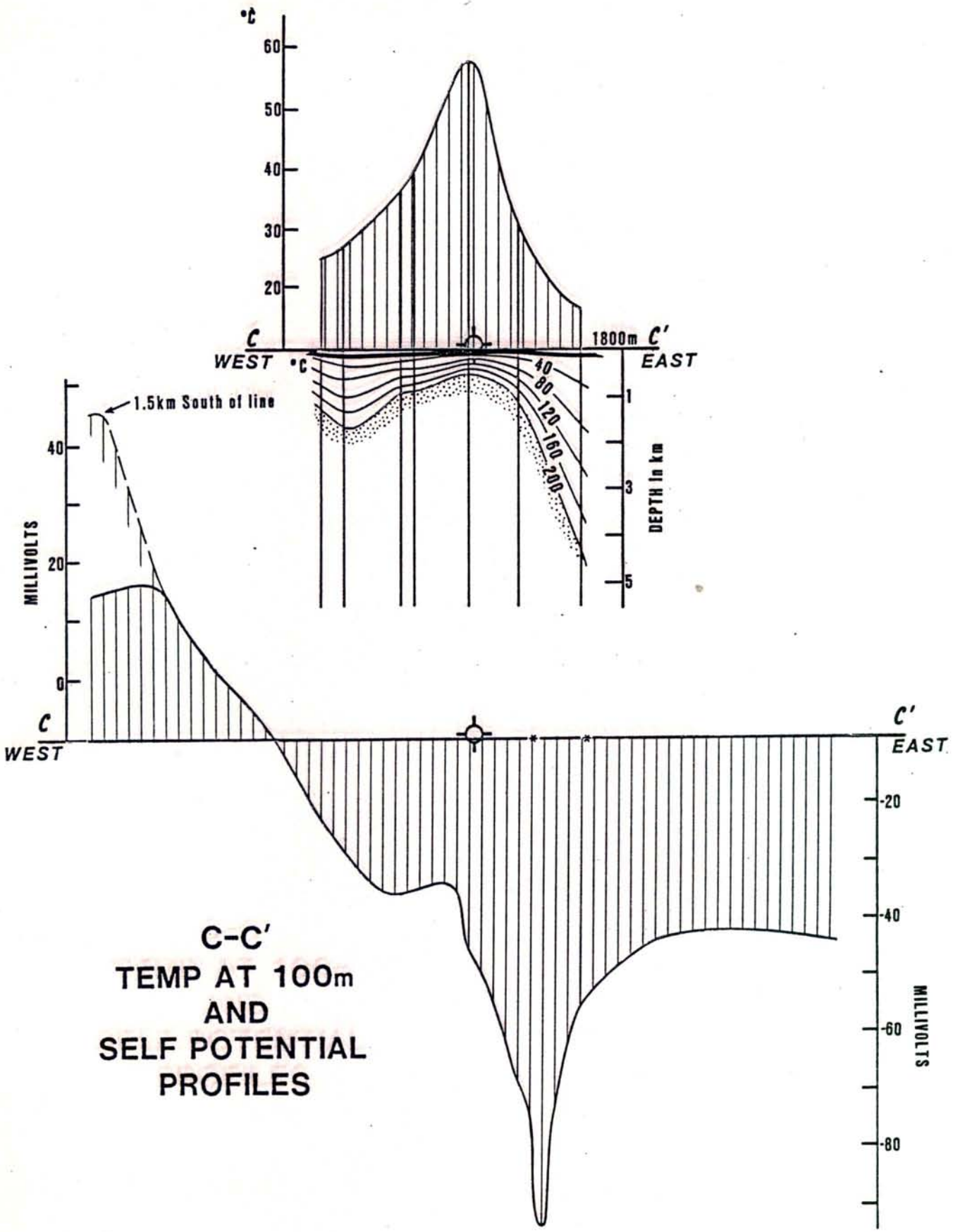


26R. Self-potential profile, Line C, compared with profile of temperature at 100m and isotherms. Microearthquake epicenters shown as stars

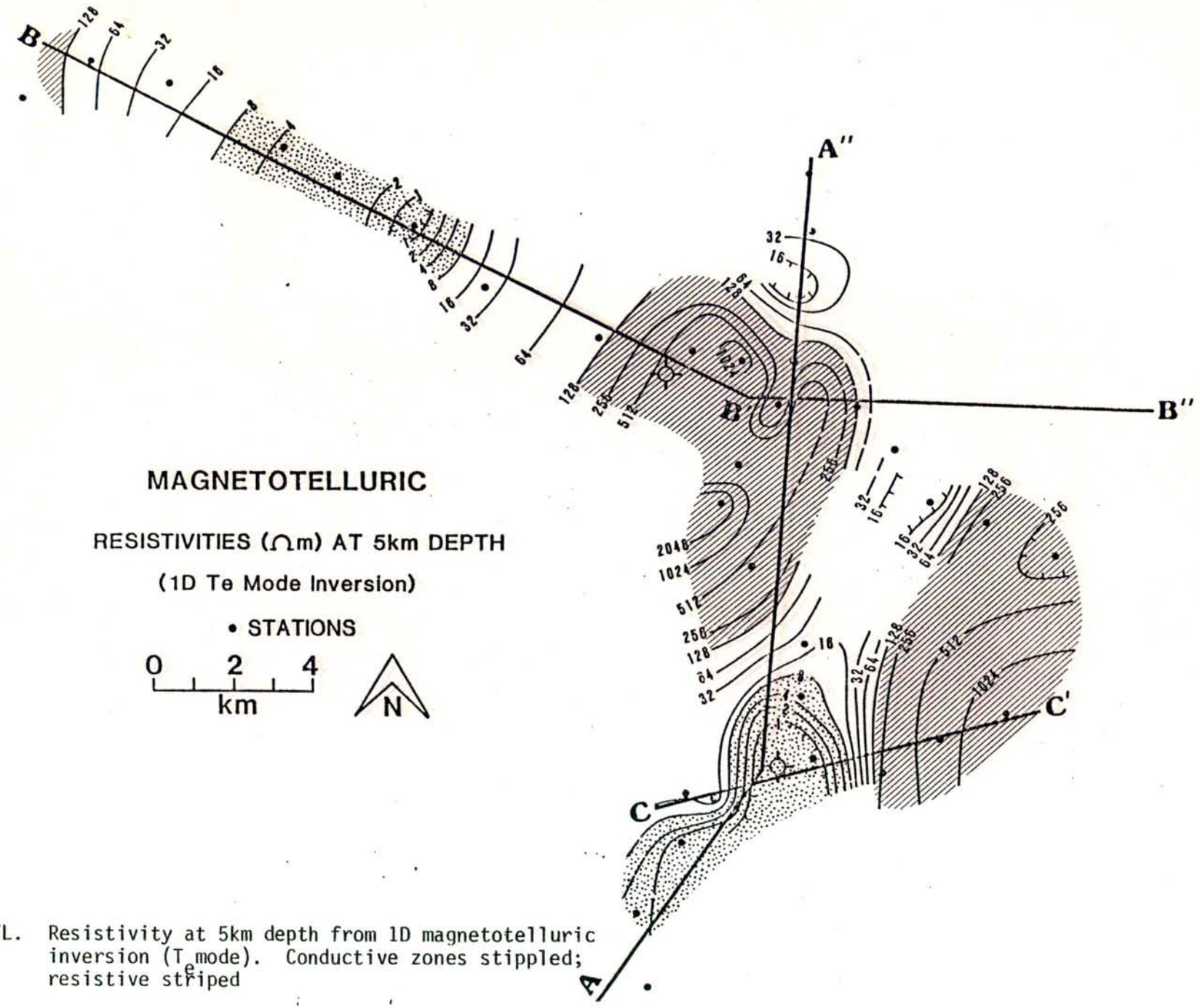


27L. Resistivity at 5km depth from 1D magnetotelluric inversion ($T_e$ mode). Conductive zones stippled; resistive striped

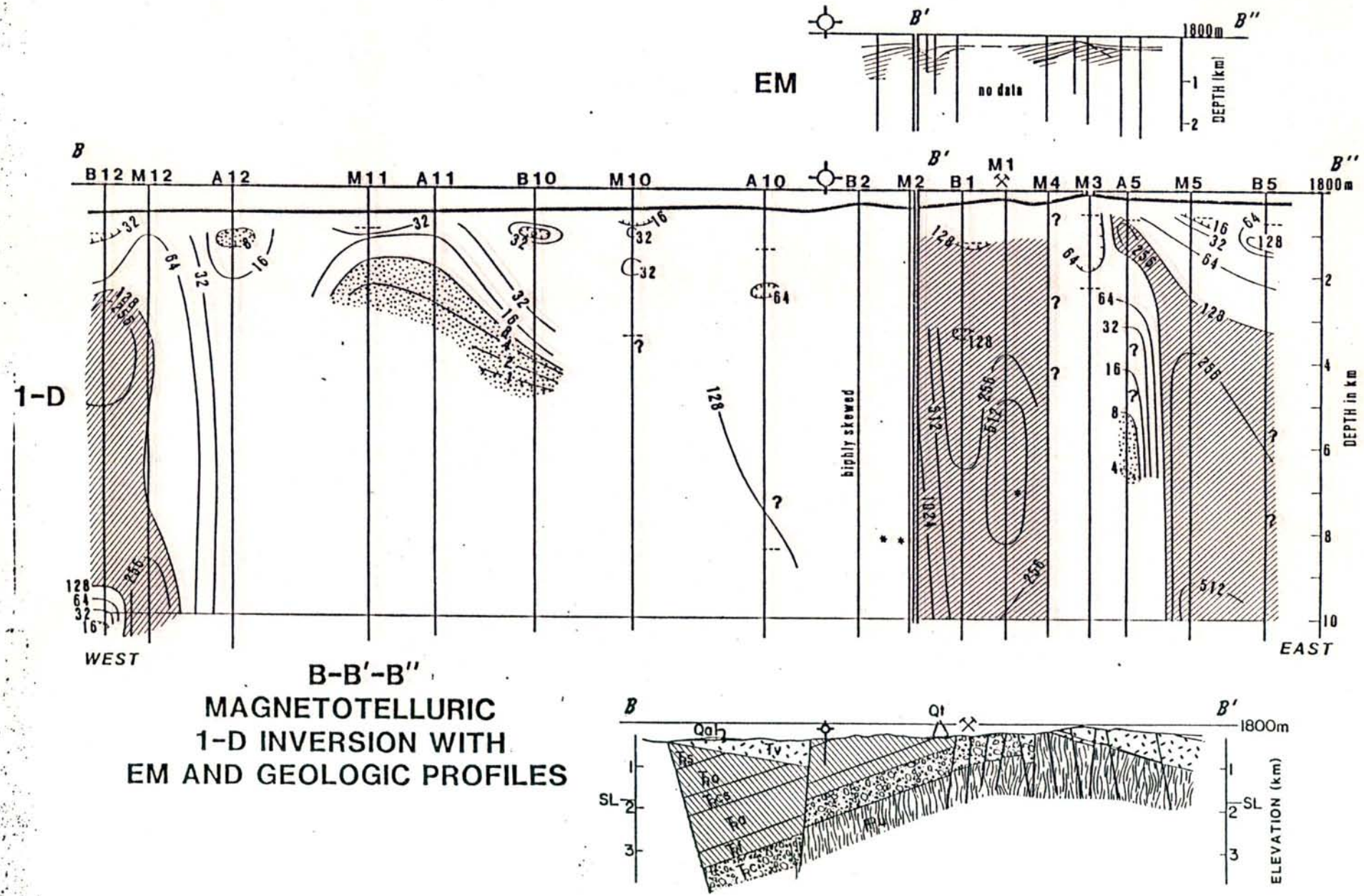


28R. Magnetotelluric section ($T_e$ mode, 1D inversion) along Line B compared with available EM section and geology

# MAGNETOTELLURIC 1-D INVERSION WITH EM PROFILE
## A-A'-A"

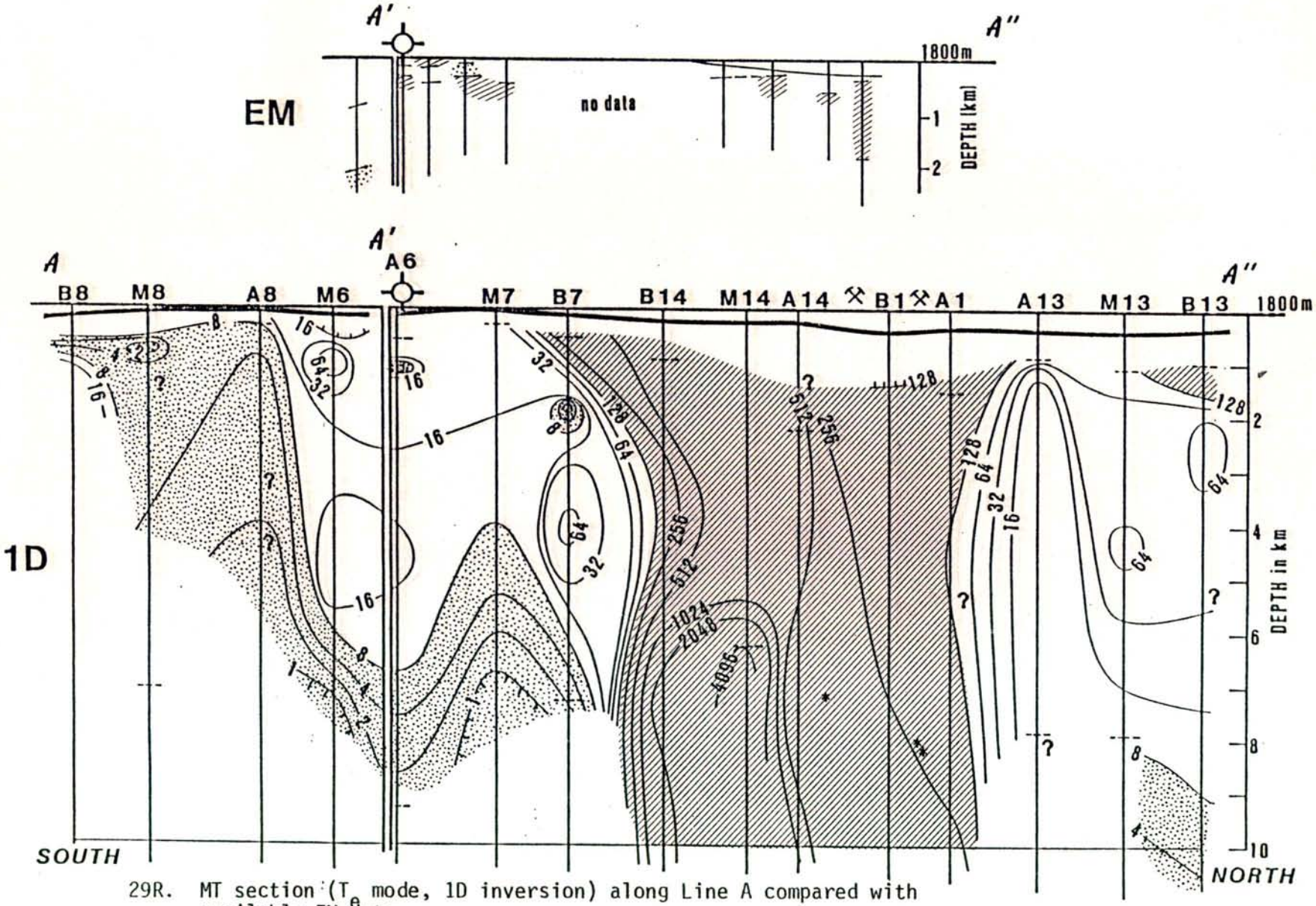


29R. MT section ($T_e$ mode, 1D inversion) along Line A compared with available EM data

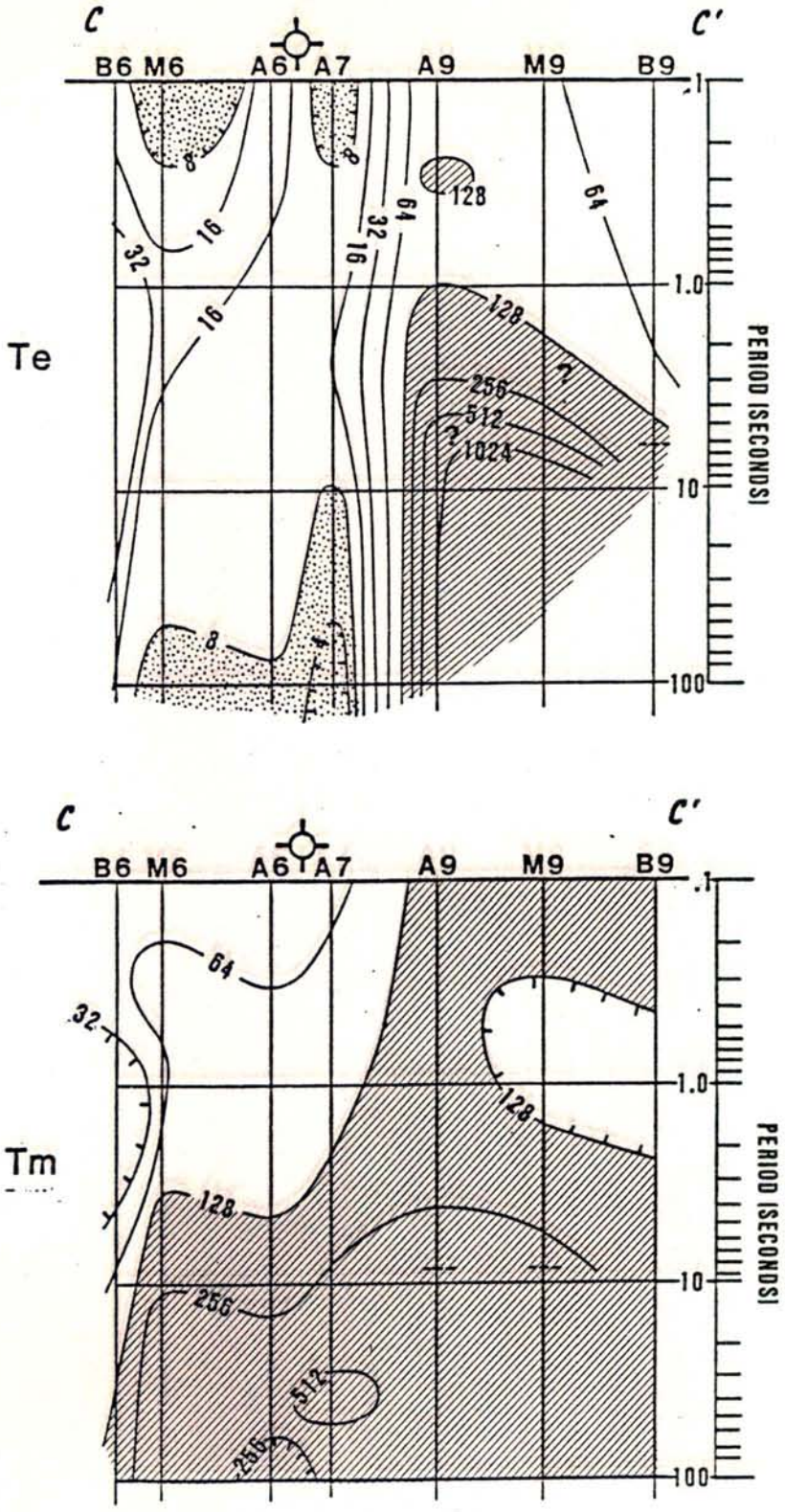


# C-C'
# MAGNETOTELLURIC PSEUDOSECTION

30R. MT pseudosections (resistivity vs. period) along Line C

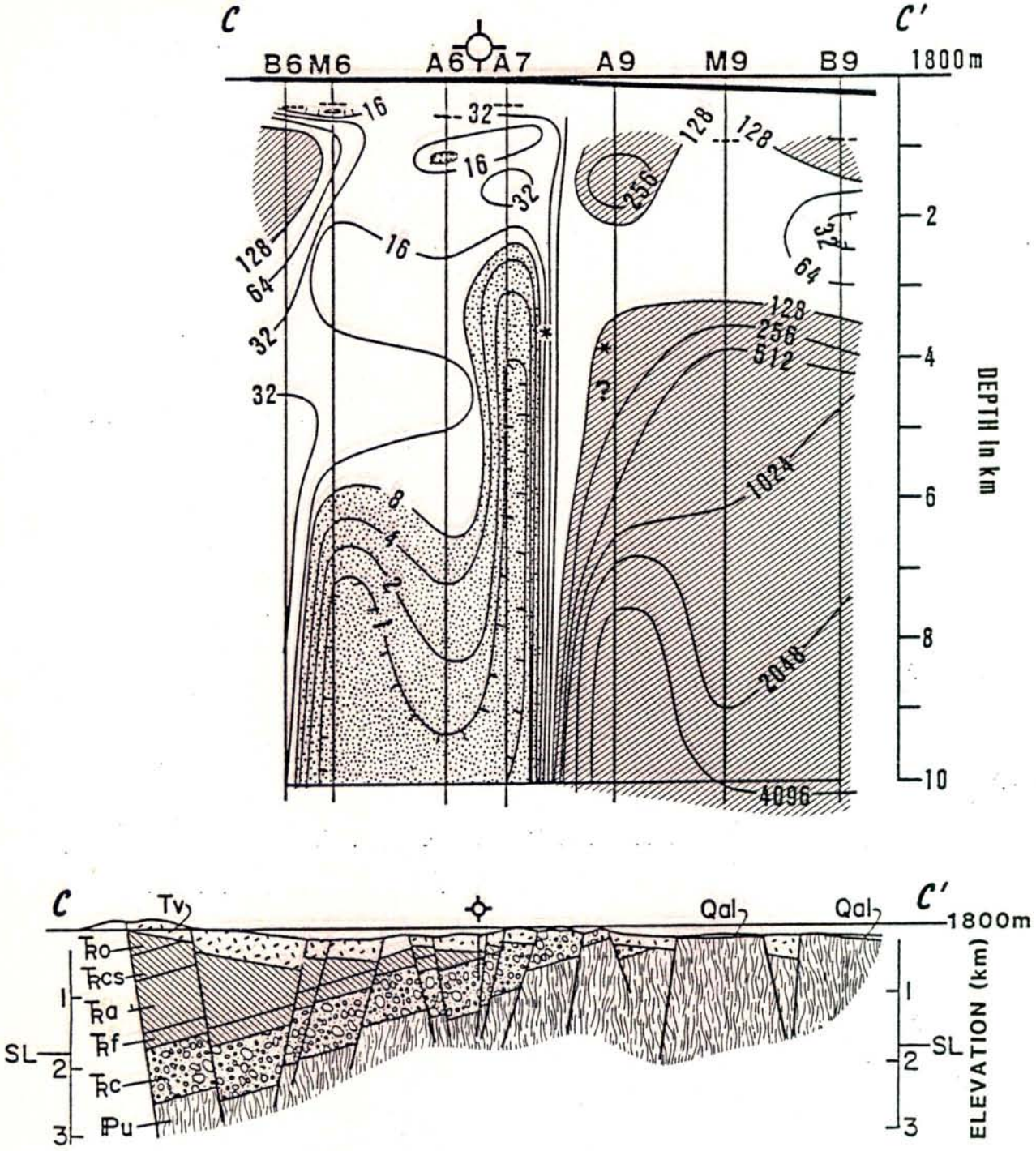


# C-C′
# MAGNETOTELLURIC 1-D INVERSION WITH GEOLOGIC PROFILE

31R. MT section ($T_e$ mode, 1D inversion) along Line C, compared with geologic section

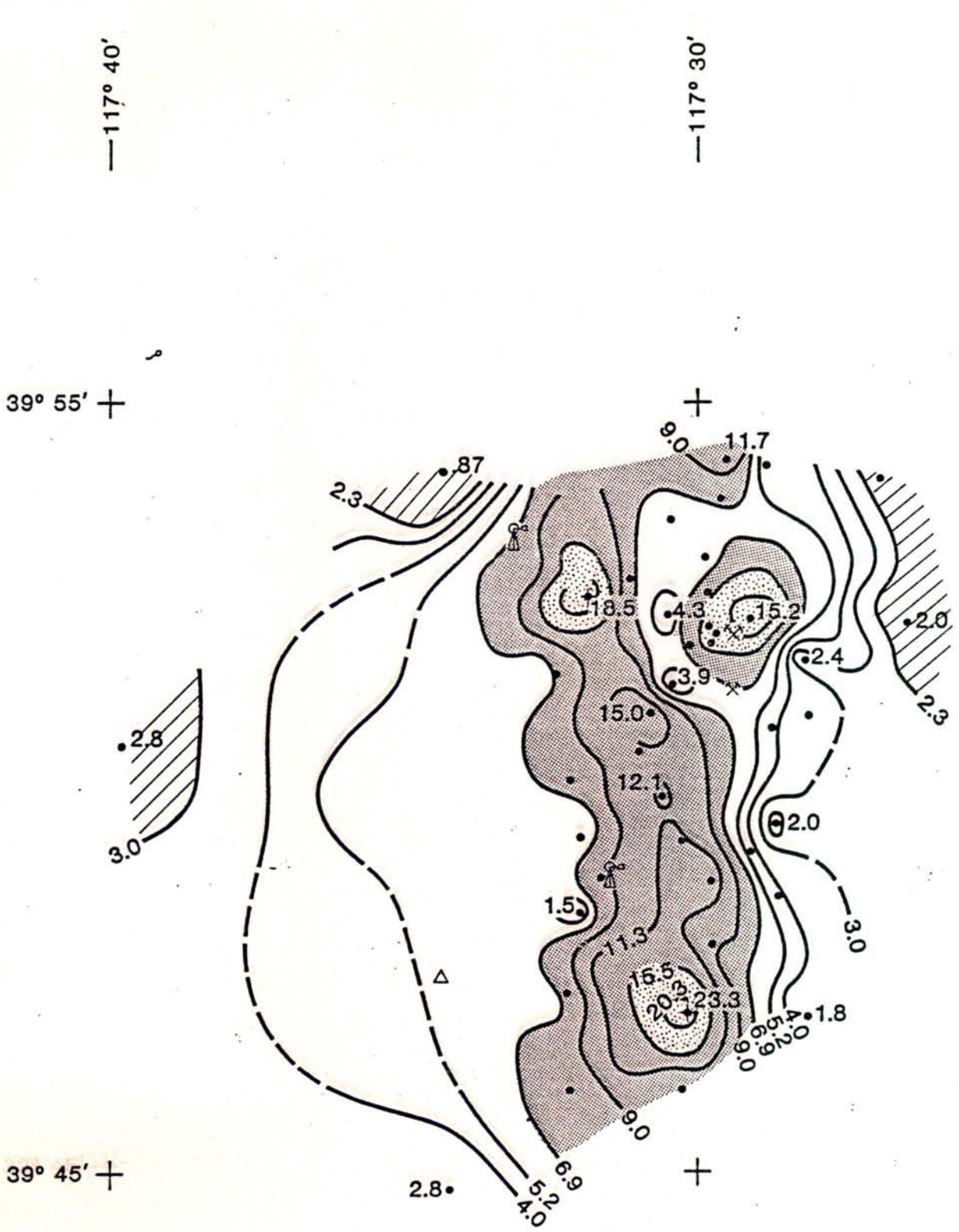


32L. Refer to Figure 8L

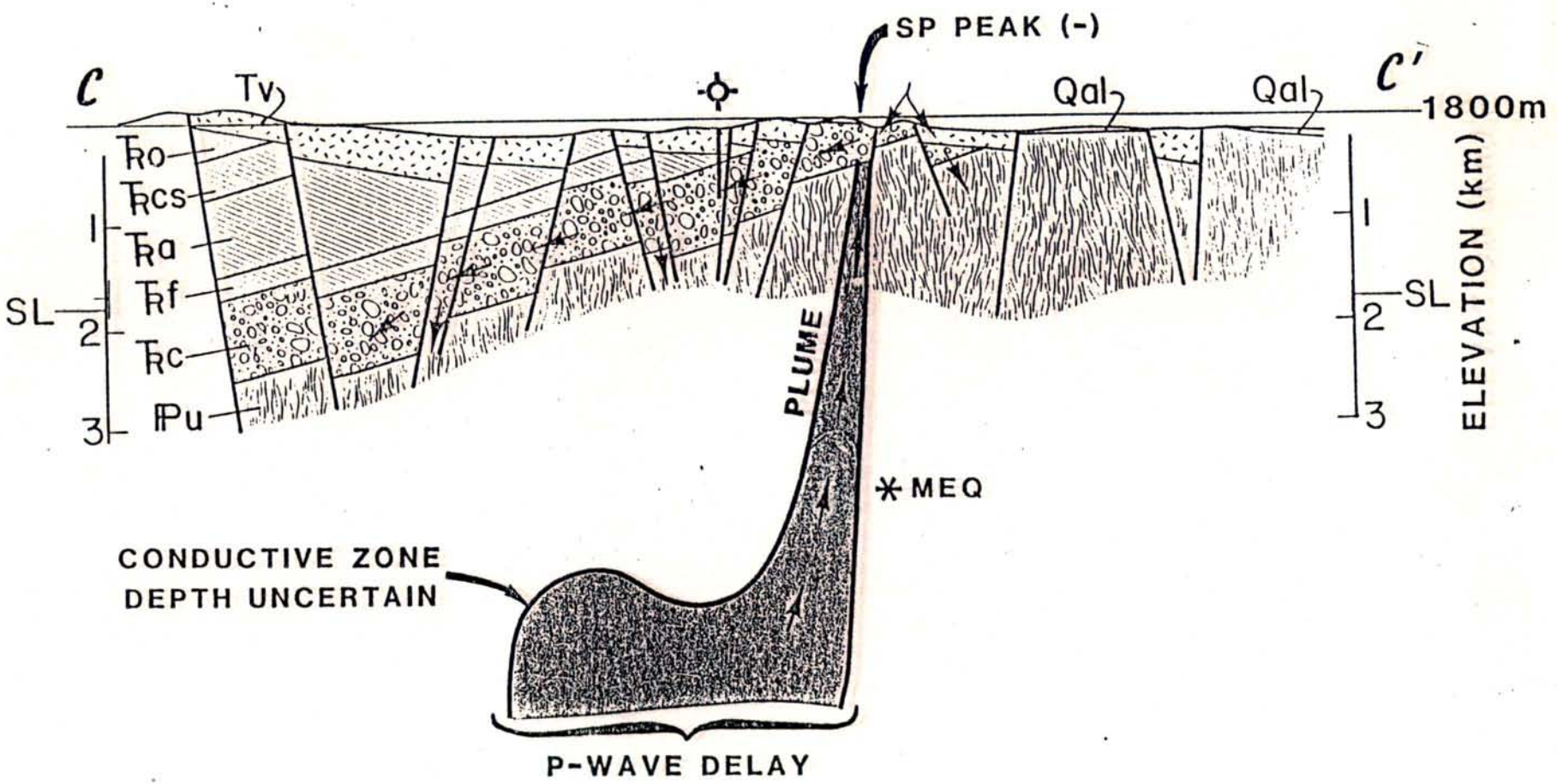


33R. Geologic section along Line C, showing deduced geothermal reservoir feeding conduit of ascending hot water along limb of horst block. Upon encountering the Triassic conglomerate, hot water (probably cooled by cold meteoric water from the surface) drains westward--downdip--to eventually return to the deep system.